1.C

Nuclear Physics **A260** (1976) 27—76, © *North-Holland Publishing Co, Amsterdam*

APPLICATION OF THE NUCLEAR FIELD THEORY TO MONOPOLE INTERACTIONS WHICH INCLUDE ALL THE VERTICES OF A GENERAL FORCE

D R. BÈS †

Cómisión Nacional de Energía Atómica, Buenos Aires, Argentina ††

R. A BROGLIA

Niels Bohr Institute, University of Copenhagen, Denmark

and

G G DUSSEL †, R J LIOTTA and H M. SOFÍA

Comisión Nacional de Energía Atómica, Buenos Aires, Argentina ††

Received 20 June 1975

Abstract: The field treatment is applied to the monopole pairing and monopole particle-hole interactions in a two-level model All the vertices of realistic interactions appear, and the problems treated here have most of the complexities of real nuclei Yet, the model remains sufficiently simple, so that a close comparison with the results of a (conventional) treatment in which only the fermion degrees of freedom are considered is possible. The applicability to actual physical situations appears to be feasible, both for schematic or realistic forces The advantage of including the exchange components of the interaction in the construction of the phonon is discussed.

1. Introduction

In this paper, we apply the field††† treatment [1]) of the residual nuclear interaction to the case of particles moving in two levels and coupled by monopole pairing and particle-hole forces. We consider cases in which these interactions generate collective excitations, but do not produce either a stable "shape" deformation or a superconducting gap. The description of the system is performed by treating the single-particle and the collective variables on an equal footing. Therefore, the basic set of states is the product of the eigenfunctions corresponding to these two degrees of freedom. The field treatment provides a systematic way to correct the errors inherent to this basis:

† Fellow of the Consejo Nacional de Investigaciones Científicas y Técnicas, Argentina

†† Mailing address: Departamento de Física Nuclear, CNEA. Avda. del Libertador 8250, Buenos Aires, (S. 29), Argentina.

††† The ubiquitous appearence of the problem of collective and quasiparticle degrees of freedom in nuclear physics has stimulated a great variety of theoretical approaches The best known among them are based on boson expansions, the Landau theory of Fermi liquids and the self-consistent equations of motion. For a recent review of the field see ref [5]), and references quoted therein The connection between the present field treatment and other particle-phonon interaction treatments is briefly discussed in the introduction of ref [2]), where previous references are also given

violations of the Pauli principle, overcompleteness, effects of the residual interaction which are not taken into account in the construction of the phonons, etc

The main difference between the present paper and ref [3]) is that here we treat problems with more realistic features† and which, correspondingly, do not permit a closed algebraic solution, neither within the field treatment, nor using the usual fermion treatments. The most simple of these problems arises in the case of a pairing interaction with both the RPA vertices given in figs 1.1 and 1.2. This first problem is used to illustrate the application of the rules for the diagrammatic expansion of the field Hamiltonian We also discuss in this case the meaning of the basic set of states, the interpretation of the diagrams, etc.

For the monopole particle-hole force, we complicate the problem by including in addition to the RPA vertices shown in figs. 11.1 and 11 2, (i) the "scattering" vertices of figs. 11.3 and 11.4, (ii) the particle-particle and hole-hole vertices (figs. 11 6 and 11.7) and (iii) the exchange components of the interaction (fig. 11.5) These last vertices may (or may not) be taken into account in the definition of the phonon A discussion of the relative advantages of these two procedures is presented All the usual complexities of real nuclei are included in this second problem. The large number of diagrams to be taken into account gives us a preview on the feasibility of the order to which the field calculations may be performed in realistic cases.

On the other hand, the model remains sufficiently simple, so that it is possible to closely compare the results of the field diagrammatic expansion with those of a pure fermion treatment of the residual interaction ††. We compare magnitudes which are algebraically obtained. In spite of the nonexistence of a closed solution, this is still possible in the present case, since there only are two dimensionless parameters in the model, and any physical quantity Y can be obtained as a double series in powers of these parameters We choose them to be (i) $1/\Omega$, where 2Ω is the degeneracy of each single-particle level and (ii) the ratio $x = \eta\Omega/\varepsilon$ where η is proportional to the strength of the residual interaction and ε is the distance between the two levels

$$Y = \sum_{n,m} a_{n,m}(x^n/\Omega^m). \tag{1 1}$$

A perturbative fermion treatment corresponds to an expansion in powers of x Thus, each column in the matrix representing the coefficients $a_{n,m}$ of (1.1) is obtained with increasing difficulty as n increases. However, all the elements in the same column are simultaneously obtained In the field diagrammatic expansion, each graph contributes to a certain order in Ω^{-1}, and thus an increase in the order of perturbation represents an increase in the power of Ω^{-1} which is taken into account Thus, the field treatment yields the succesive rows of coefficients $a_{n,m}$ with increasing difficulty, but all the elements in the same row with equal facility In particular,

† The problem of particles coupled through a pairing and monopole forces having only the TDA vertices is treated in ref [3])

†† We have avoided using the numerical similarity between two curves as an argument for the verification of the equivalence between the two treatments The validity of these visual arguments is handicapped by their dependence on the scale, range of parameters, etc

the RPA is the exact solution in the limit of infinite degeneracy, and thus it gives all the coefficients $a_{n,0}$ (n arbitrary)

In consequence, the usefulness of the two perturbative treatments becomes complementary to each other. In the present paper, we obtain the first columns of some matrices ($a_{n,m}$) through the fermion perturbation, and the first rows of the same matrices through the field treatment. We verify that the two treatments give identical coefficients for the corresponding regions of overlap

The present paper has also a pedagogical aim: to perform an application as clear as possible of the diagrammatic rules [1]) of the field treatment of a two-body interaction H_{tb}. As previously mentioned, one uses the product space of the wave functions representing independent particle and independent phonons as the basic set of states Consequently, we take into account both fermion and boson terms in the field Hamiltonian and other field operators. The fermion terms include a single-particle Hamiltonian H_{sp} (which contains the Hartree-Fock contributions from H_{tb}) and the original interaction H_{tb} (minus the Hartree-Fock contributions). The boson parameters must be consistent with the initial two-body interaction The most practical way to derive these parameters is through an RPA calculation Thus, we obtain the frequencies of the phonons and the amplitudes λ, μ [eqs. (2 14), (3 18), (3.40) and (3 43)] which determine the value of the particle-vibration vertices [eqs (2 16), (3.20), (3 47) and (3 48)] and the phonon terms in the transition operators [eqs. (2.33) and (3 26)] The total field Hamiltonian [eqs. (2 20) and (3.23)] and field operators are treated within a graphical perturbation expansion This is necessary, since one must disregard all diagrams in which a pair of particles (holes) interact twice with each other, through the same two-body vertices (figs. 1.1 and 1.2) entering in the RPA calculation and/or through particle-vibration vertices (figs 2 1 and 2 2) Of course, if any of the two lines interact in between with a third line, the diagram should be maintained. A similar rule holds for diagrams including interactions between particle-hole lines, in the case of particle-hole collective modes The remaining graphs have to be evaluated according to the usual rules for the calculation of diagrams In particular, all time orderings of the vertices have to be included.

Initial and final states must be proper states, i e , states which include particle, phonons or both, but not any particle configuration which may be replaced by a combination of phonons. This restriction does not apply to intermediate states.

If in a given diagram there is a fermion line and a particle-hole boson line in parallel [such as in graph (19.1)], we must subtract another diagram in which the phonon is replaced by a pair of (non-interacting) particle-hole lines [graph (19 2)], (subsect. 3 2.2) However, this rule does not apply when only the direct terms are used in the RPA equations which determine the properties of the phonons [for instance, in the case of a separable interaction (subsect 3.2.1)].

2. The pairing force Hamiltonian in the two-level model

2 1 FERMION CALCULATION

In this subsection, we discuss the pairing residual interaction. In the first place, we ensure that this interaction does not contribute to the Hartree-Fock excitation energies In addition, we perform a conventional perturbation calculation of the pairing force. The results of this calculation are given in table 1, for various physical magnitudes. The pairing interaction is treated within the field formalism in subsect 2 2.

We start with a fermion Hamiltonian H which includes a single-particle term $H_{s\,p}$ and a two-body interaction † H_p,

$$H = H_{s\,p} + H_p, \tag{2.1}$$

$$H_{s\,p} = \tfrac{1}{2}\varepsilon_0(N_1 + N_{\bar{1}}), \tag{2.2}$$

$$H_p = -\tfrac{1}{2}G(P^+P + PP^+), \tag{2.3}$$

where

$$P^+ = A_1^+ + A_{\bar{1}}, \tag{2.4}$$

$$\begin{aligned} A_1^+ &= \sum_{m>0} c_{m1}^+ c_{\bar{m}1}^+, \qquad N_1 = \sum_m c_{m1}^+ c_{m1}, \\ A_{\bar{1}}^+ &= \sum_{m>0} c_{\bar{m}\bar{1}} c_{m\bar{1}}, \qquad N_{\bar{1}} = \sum_m c_{m\bar{1}} c_{m\bar{1}}^+. \end{aligned} \tag{2 5}$$

The operator $c_{m\sigma}^+$ creates a particle in the state (m, σ). The subindex $\sigma = 1$ or $\sigma = -1 = \bar{1}$ denotes the upper and lower level, respectively Each level has degeneracy 2Ω and the semi-integer number m ($|m| \leqq \Omega - \frac{1}{2}$) labels the degenerate states The state $(\bar{m}, \sigma) = (-m, \sigma)$ is the time reversal state of (m, σ). The quantity ε_0 is the distance between the two levels and G, the strength of the pairing interaction

The interaction (2 3) satisfies the Hartree-Fock condition for the closed-shell system, namely the vanishing of the matrix elements of H between the vacuum state and particle-hole states. Therefore, no change is required for the wavefunction of the single-particle states $c_{m1}^+|\mathrm{HF}\rangle$ and single-hole states $c_{m\bar{1}}|\mathrm{HF}\rangle$.

However, there is a contribution of H_p (2.3) to the Hartree-Fock energies ε_σ, which are defined through the linearization equations

$$\begin{aligned} [H, c_{m1}^+]|\mathrm{HF}\rangle &= \varepsilon_1 c_{m1}^+|\mathrm{HF}\rangle, \\ [H, c_{m\bar{1}}]|\mathrm{HF}\rangle &= -\varepsilon_{\bar{1}} c_{m\bar{1}}|\mathrm{HF}\rangle \end{aligned} \tag{2 6}$$

Here $|\mathrm{HF}\rangle$ is the closed shell Hartree-Fock vacuum ‡,

$$c_{m1}|\mathrm{HF}\rangle = c_{m\bar{1}}^+|\mathrm{HF}\rangle = 0. \tag{2.7}$$

† The difference between (2 3) and the more conventional form $H_p = -GP^+P$ is a term which is proportional to the number of particles and which therefore simply displaces by equal amounts all the levels belonging to the same system

‡ Note that there are several ground or vacuum states used in the text, and a clear distinction between them has to be made Here $|\mathrm{HF}\rangle$ is the closed shell ground state in which all levels with $\sigma = \bar{1}$ are occupied and those with $\sigma = 1$ are empty, ($c_{m1}|\mathrm{HF}\rangle = c^+{}_{m\bar{1}}|\mathrm{HF}\rangle = 0$), $|\psi\rangle$ is the RPA ground state ($\Gamma_n|\psi\rangle = 0$ where Γ_n is the phonon annihilation operator); $|0\rangle$ is the vacuum state in the field treatment ($c_{m1}|0\rangle = c^+{}_{m\bar{1}}|0\rangle = \Gamma_n|0\rangle = 0$); $|\mathrm{g.s}\rangle$ is the exact ground state, which is obtained by treating the interaction in all order of perturbations; and $|\mathrm{v}\rangle$ is the vacuum state for all particles

Introducing (2.1) in (2.6), we obtain

$$\varepsilon_1 = -\varepsilon_{\bar{1}} = \tfrac{1}{2}(\varepsilon_0 + G). \tag{2.8}$$

Therefore, the particle-hole, Hartree-Fock excitation energy ε is given as

$$\varepsilon = \varepsilon_1 - \varepsilon_{\bar{1}} = \varepsilon_0 + G. \tag{2.9}$$

We redistribute the terms (2.2) and (2.3) in (2.1) so as to include in $H'_{s\,p}$ the Hartree-Fock contributions of H_p,

$$\begin{aligned} H &= H'_{s\,p} + H'_p, \\ H'_{s\,p} &= \tfrac{1}{2}\varepsilon(N_1 + N_{\bar{1}}), \\ H'_p &= -\tfrac{1}{2}G(P^+P + PP^+ + N_1 + N_{\bar{1}}). \end{aligned} \tag{2.10}$$

The same vertices (fig. 1) correspond to the residual interactions H_p and H'_p

In a Feynman perturbation expansion corresponding to H'_p, diagrams containing Hartree-Fock insertions vanish. The same vertices (fig. 1) correspond to the residual interaction H_p and H'_p. The values of these vertices are †

$$(m_3\sigma_3, m_4\sigma_4|\bar{H}'_p|m_2\sigma_2; m_1\sigma_1) = -G\delta_{m_4,\bar{m}_3}\delta_{\sigma_4,\sigma_3}\delta_{m_1,\bar{m}_2}\delta_{\sigma_1,\sigma_2} \qquad (m_2, m_3 > 0) \tag{2.11}$$

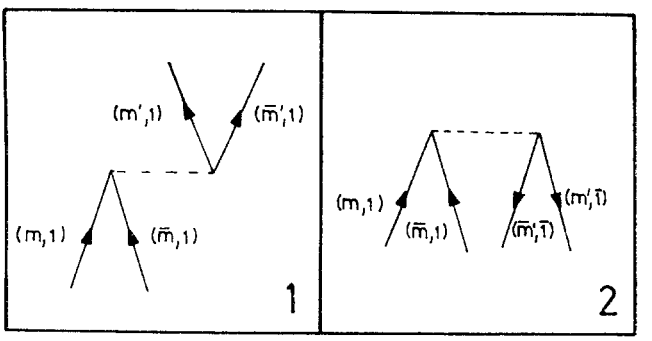

Fig 1 The vertices corresponding to the two-body pairing interaction In each graph there are two pairs of fermion lines The fermions belonging to the same pair meet the vertex at the same point The value of these vertices is $-G$ if in each pair of particle lines, the one corresponding to the state $m > 0$ appears to the left of $\bar{m} < 0$, and if in each pair of hole lines, the line corresponding to $\bar{m} < 0$ is placed to the left of $m > 0$ (as in the figure). A minus sign appears for each interchange of this order.

If $\sigma_3 = \sigma_2 = 1$, the vertex (2 11) corresponds to fig. 1.1; if $\sigma_3 = -\sigma_2$, to fig 1 2.

The most general matrix elements of H'_p are constructed in appendix A. Use is made of the quasispin formalism, in a representation carrying N_1 and $N_{\bar{1}}$ as good

† The bar on top of H_p' [eq (2 11)] indicates antisymmetrized two-body matrix elements, $(m_3\sigma_3, m_4\sigma_4|\bar{H}_p'|m_2\sigma_2, m_1\sigma_1) = -(m_3\sigma_3; m_4\sigma_4|\bar{H}_p'|m_1\sigma_1; m_2\sigma_2)$, although the graphical representation of fig 1 is that usually employed for the direct component of the interaction

TABLE

The fermion calculation of the coefficients $a_{n,m}$ for several energies

n	$E(\mathbf{P})-E(\text{g.s.})$			$E(\mathbf{F})-E(\text{g.s.})$			$E(\mathbf{1})-E(\mathbf{P})-E(\mathbf{F})$		
	a_{n0}	a_{n1}	a_{n2}	a_{n0}	a_{n1}	a_{n2}	a_{n0}	a_{n1}	a_{n2}
0	128			64					
1	−64								
2	−16	32			16			16	−32
3	− 8	32	−16		12	− 4		12	−44
4	− 5	36	−48		10	−12			

quantum numbers. These matrix elements are used in perturbation theory, in order to obtain energies and transition matrix elements. The results are straightforward but tedious to obtain They are cast into the form (1 1) with

$$x = 2G\Omega/\varepsilon \tag{2.12}$$

The resultant matrix elements $a_{m,n}$ are given in table 1 for six cases of interest. Three of them correspond to excitation energies The fourth, to the energy of the closed shell system, and the last two are the matrix elements of the operators $A_1^+, A_{\bar{1}}$, which create two particles in the upper and lower single-particle states, respectively. The symbols* (g.s.) and (**P**) label the lowest state of the closed shell system and of the system with two more particles, respectively In the odd nucleus, with one particle more than the closed shell, (**F**) denotes the lowest state while (**1**) indicates the first excited state Both (**F**) and (**1**) have a degeneracy of order 2Ω.

2 2 NUCLEAR FIELD CALCULATION OF THE PAIRING INTERACTION

2.2.1 Construction of the pairing field Hamiltonian. As is shown in ref. [2]), the phonon terms in the field Hamiltonian are conveniently (but not necessarily) defined through the RPA equations In the pairing case, there are two vibrational modes, the addition ($\sigma = 1$) and the removal ($\sigma = \bar{1}$) modes Since the interaction is separable, the phonon frequencies are given as roots of a simple dispersion equation There is a single root $\omega = \omega_1 = \omega_{\bar{1}}$ different from ε, because of the particular degeneracies of our problem,

$$\omega = \varepsilon(1-x)^{\frac{1}{2}}, \tag{2.13}$$

where x is given in (2.12). The RPA also yields the matrix elements

$$\begin{aligned} \langle\psi_1|A_1^+|\psi\rangle &= \langle\psi_{\bar{1}}|A_{\bar{1}}^+|\psi\rangle = \Omega\lambda = \tfrac{1}{2}(\varepsilon+\omega)(\Omega/\varepsilon\omega)^{\frac{1}{2}}, \\ \langle\psi_1|A_{\bar{1}}|\psi\rangle &= \langle\psi_{\bar{1}}|A_1|\psi\rangle = \Omega\mu = \tfrac{1}{2}(\varepsilon-\omega)(\Omega/\varepsilon\omega)^{\frac{1}{2}}, \end{aligned} \tag{2.14}$$

where $|\psi_\sigma\rangle$ represents the RPA state with one σ-phonon present and $|\psi\rangle$ is the RPA ground state.

Eqs (2 13) and (2.14) constitute all the results that we must obtain through the

* (**P**) ≡ (↑↑) , (**F**) ≡ (↑) ,
(**1**) ≡ (↓ ↑↑) , (**S**) ≡ (↕)

1

and matrix elements, in units of $\frac{1}{128}$ (pairing interaction)

E(g s)			$\langle \mathbf{P}\|A_1^+\|$g s$\rangle$			$\langle \mathbf{P}\|A_{-1}\|$g s$\rangle$		
a_{n0}	a_{n1}	a_{n2}	a_{n0}	a_{n1}	a_{n2}	a_{n0}	a_{n1}	a_{n2}
			128					
−64						32		
−16			4	−8		16		
− 8			4	−8		11	−14	8
− 5	4	−2						

RPA in order to construct the collective field Hamiltonian.

The term of the field Hamiltonian representing the set of independent phonons is

$$H_b = \omega(\Gamma_1^+\Gamma_1 + \Gamma_{\bar{1}}^+\Gamma_{\bar{1}}), \tag{2.15}$$

where Γ_σ^+ is the creation operator for a σ-phonon.

The particle-vibration interaction vertices are given in ref. [2]). For the addition mode,

$$\begin{aligned}
\Lambda_1(m_1 1; m_2 1) &= \langle n_1 = 1|H_{\mathrm{p\,v}}\, c_{m_1 1}^+ c_{m_2 1}^+|0\rangle \\
&= \sum_{\substack{m>m' \\ \sigma}} (m_1 1, m_2 1|\bar{H}'_{\mathrm{p}}|m\sigma; m'\sigma)\langle\psi|c_{m'\sigma} c_{m\sigma}|\psi_1\rangle \\
&= \delta_{m_2,\bar{m}_1} \sum_{\substack{m>0 \\ \sigma}} (m_1 1; \bar{m}_1 1|\bar{H}'_{\mathrm{p}}|m\sigma; \bar{m}\sigma)\langle\psi|c_{\bar{m}\sigma} c_{m\sigma}|\psi_1\rangle \\
&= -\Lambda\delta_{m_2,\bar{m}_1} \qquad \text{(fig 2.1)}, \\
\Lambda_1(m_1 \bar{1}; m_2 \bar{1}) &= \langle 0|H_{\mathrm{p\,v}}\, c_{m_2\bar{1}}\, c_{m_1\bar{1}}|n_1 = 1\rangle \\
&= \sum_{\substack{m>m' \\ \sigma}} (m_1 \bar{1}; m_2 \bar{1}|\bar{H}'_{\mathrm{p}}\, m\sigma, m'\sigma)\langle\psi|c_{m\sigma} c_{m\sigma}|\psi_1\rangle \\
&= -\Lambda\delta_{m_2,\bar{m}_1} \qquad \text{(fig 2.2)}, \\
\Lambda_1(m_1 1; m_2 \bar{1}) &= \langle 0|c_{m_1 1}\, H_{\mathrm{p\,v}}\, c_{m_2\bar{1}}|n_1 = 1\rangle \\
&= \sum_{\substack{m>m' \\ \sigma}} (m_1 1; m_2 \bar{1}|\bar{H}'_{\mathrm{p}}|m\sigma, m'\sigma)\langle\psi|c_{m\sigma} c_{m\sigma}|\psi_1\rangle \\
&= 0 \qquad \text{(fig 2.3)}.
\end{aligned} \tag{2.16}$$

Use has been made of (2.11). Here, $|0\rangle$ is the vacuum state in the field treatment

and $|n_\sigma\rangle$ is the state with n_σ σ-phonons. The constant Λ in (2.16) has the value

$$\begin{aligned}\Lambda &= -\sum_{\substack{m>0\\ \sigma}} (m_1\sigma_1; \bar{m}_1\sigma_1|\bar{H}'_{\mathrm{p}}|m\sigma; \bar{m}\sigma)\langle\psi|c_{\bar{m}\sigma}c_{m\sigma}|\psi_1\rangle \\ &= G(\langle\psi|A_1|\psi_1\rangle+\langle\psi|A_{\bar{1}}^{+}|\psi_1\rangle) \\ &= G\sqrt{\Omega}(\lambda+\mu) = G(\Omega\varepsilon/\omega)^{\frac{1}{2}} \\ &= \tfrac{1}{2}\varepsilon x(\varepsilon/\omega\Omega)^{\frac{1}{2}}. \end{aligned} \tag{2.17}$$

We proceed similarly for the removal phonon

$$\begin{aligned}\Lambda_{\bar{1}}(m_1 1; m_2 1) &= \langle 0|H_{\mathrm{p\,v.}}c_{m_1 1}^{+}c_{m_2 1}^{+}|n_{\bar{1}}=1\rangle = -\Lambda\delta_{m_2,\bar{m}_1}, \\ \Lambda_{\bar{1}}(m_1\bar{1}; m_2\bar{1}) &= \langle n_{\bar{1}}=1|H_{\mathrm{p\,v}}\,c_{m_2\bar{1}}c_{m_1\bar{1}}|0\rangle = -\Lambda\delta_{m_2,\bar{m}_1}, \\ \Lambda_{\bar{1}}(m_1 1; m_2\bar{1}) &= \langle 0|c_{m_2\bar{1}}^{+}H_{\mathrm{p.v.}}c_{m_1 1}^{+}|n_{\bar{1}}=1\rangle = 0. \end{aligned} \tag{2.18}$$

The sign on the right-hand side of eqs. (2.16) and (2 18) corresponds to the case $m_1 > 0$.

All the interaction vertices for the addition and removal phonons have the same value, $-\Lambda$, and the selection rule, $\delta_{m_1,\bar{m}_2}\delta_{\sigma_1,\sigma_2}$. This selection rule implies that the two-fermion lines joining a given vertex, should correspond either to two particles

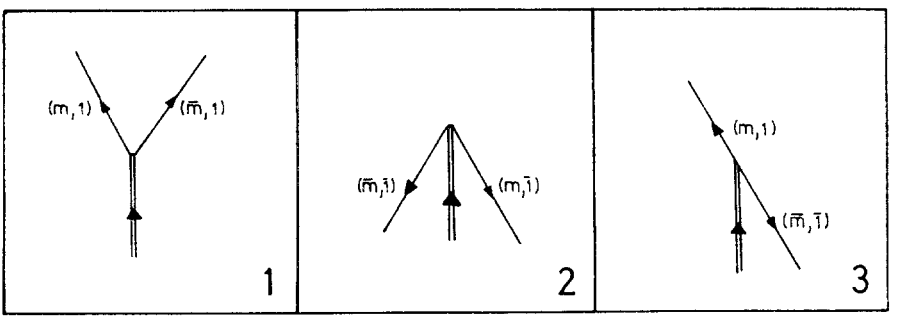

Fig 2. Vertices corresponding to the particle-vibration interaction. The value of the vertices 2 1 and 2.2 is $-\Lambda$ if the particle line corresponding to $m > 0$ appears to the left of the particle line $\bar{m} < 0$, or the hole line corresponding to $\bar{m} < 0$ is placed to the left of the hole line corresponding to $m > 0$ A minus sign appears for an interchange of this order Similar vertices exist for the removal phonons

or two holes. In consequence, only the vertices 2 1 and 2 2 have the value $-\Lambda$, while 2 3 vanishes (fig. 2)

The particle-vibration interaction $H_{\mathrm{p\,v}}$ is written

$$H_{\mathrm{p\,v}} = -\Lambda((\Gamma_1^{+}+\Gamma_{\bar{1}})(A_1+A_{\bar{1}}^{+})+(\Gamma_1+\Gamma_{\bar{1}}^{+})(A_1^{+}+A_{\bar{1}})). \tag{2.19}$$

Note that, in general, (2 15) and (2.19) include as many different phonons as roots of the RPA equations. In the present case, however, the roots other than ω

(2.13) are irrelevant, since the corresponding particle-vibration vertices (2.17) vanish and, therefore, there is no coupling (2 19) between these phonons and the remaining system.

The total field Hamiltonian H_f is made of (2.10), (2.15) and (2.19)

$$H_f = H'_{sp} + H'_p + H_b + H_{pv} . \tag{2 20}$$

This Hamiltonian must be treated within a diagramatic perturbation expansion. All diagrams in which two particles (or two holes) appear at the same vertex and, without interacting in between, together disappear at a second vertex (bubbles) must be disregarded.

2.2.2 Calculation of the energies using the field Hamiltonian The zero-order field Hamiltonian is

$$H_0 = H'_{sp} + H_b . \tag{2.21}$$

Thus, for the one-phonon state alone, or for the one-phonon state in the presence of a hole, the zero-order excitation energies are given by the RPA frequency ω [eq (2 13)]

$$E^{(0)}(\mathbf{P}) - E^{(0)}(\text{g s.}) = E^{(0)}(\mathbf{1}) - E^{(0)}(\mathbf{F}) = \omega = \varepsilon(1 - \tfrac{1}{2}x - \tfrac{1}{8}x^2 - \tfrac{1}{16}x^3 - \tfrac{5}{128}x^4 - \ldots) \tag{2.22}$$

For the single-particle state, the zero-order energy is [eq. (2.8)]

$$E^{(0)}(\mathbf{F}) - E^{(0)}(\text{g s.}) = \tfrac{1}{2}\varepsilon \tag{2 23}$$

The zero-order energy of the vacuum state has the RPA value (see appendix B)

$$E^{(0)}(\text{g.s}) = -\frac{x\varepsilon}{\varepsilon + \omega} = -\tfrac{1}{2}x\varepsilon(1 + \tfrac{1}{4}x + \tfrac{1}{8}x^2 + \tfrac{5}{64}x^3 + \ldots). \tag{2 24}$$

The values (2.22), (2.23) and (2.24) coincide with those obtained in the fermion calculation in the limit $\Omega \to \infty$ (see table 1) Thus, the coefficients $a_{n,0}$ are correctly given by the zero-order Hamiltonian (2.21). Since the graphical corrections are of higher order in Ω^{-1}, we have verified the fact that the RPA yields the exact results in the limit $\Omega \to \infty$ (if x remains smaller than unity †)

The other coefficients $a_{n,m}$ ($m \neq 0$) are given by the diagrammatic perturbation expansion In the present case, a given diagram contributes to a single power of Ω^{-1}, which is determined as follows· each factor A is proportional to $\Omega^{-\frac{1}{2}}$; each independent summation over intermediate single-particle states yields a factor 2Ω (degeneracy of the levels) and each four-point vertex, a factor $G = x\varepsilon/2\Omega = O(\Omega^{-1})$ [eq (2 12)]

Every diagram is calculated according to the usual rules [4, 3])

A diagram in which the initial (or final) state is not an intermediate state will be denoted as a BW diagram ††. If either the initial or final state is an intermediate state,

† The condition that ω is real implies $x \leqq 1$ [eq (2 13)] We also assume that the difference between ε and ω is of the same order of ε

†† BW stands for Brillouin-Wigner

it is a renormalization diagram. In the Brillouin-Wigner graphical perturbation expansion [see appendix B of ref. [3])] no renormalization diagrams occur. These diagrams are taken implicitly into account by using the exact energies of the initial or final states in the denominators of BW diagrams. In the present paper we expand these energy denominators in powers of Ω^{-1}. The zero-order term of this expansion yields the denominator of the Rayleigh-Schrödinger perturbation theory for BW diagrams. The higher-order terms correspond to Rayleigh-Schrödinger contributions from renormalization diagrams.

We apply these rules to the calculation of the four energies listed in table 1. In all these cases, there is only one graphical correction of order Ω^{-1}, which is represented in figs. 3.1, 4.1, 5.1 and 6.1, respectively.

Note that, in this paper, each drawn diagram represents also all the other diagrams which may be obtained from the first one through (i) a permutation of the time order of the vertices, and (ii) a change in the sense of the arrows corresponding to intermediate states.

As an illustration of the procedure which is used in the evaluation of diagrams, we calculate in detail the graph 3 1.

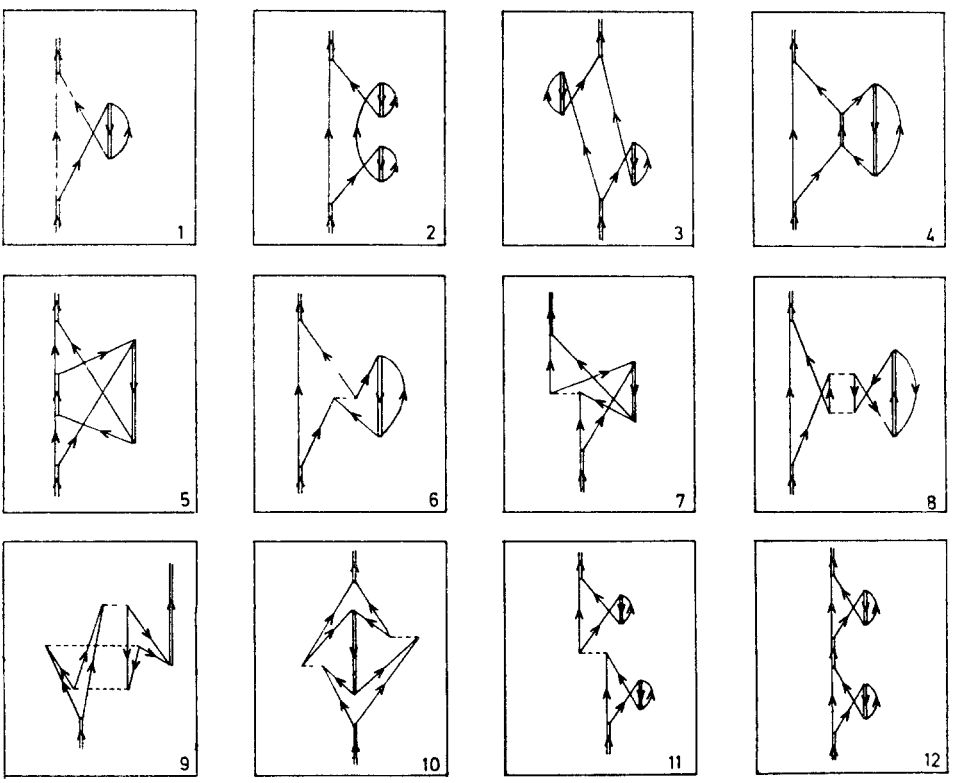

Fig 3. Diagrams contributing to the energy of the one-phonon state

If we allow for all the time permutation of the vertices, we obtain $4! = 24$ diagrams. From these, sixteen diagrams have scattering vertices which vanish. Thus, the eight diagrams given in fig. 7 remain to be evaluated.

Each diagram contributes with a factor Λ^4 (since there are four particle-vibration vertices). The summation over all intermediate particle states m introduces another factor 2Ω Thus, these diagrams contribute to the order $(\Omega^{-\frac{1}{2}})^4\,\Omega = \Omega^{-1}$.

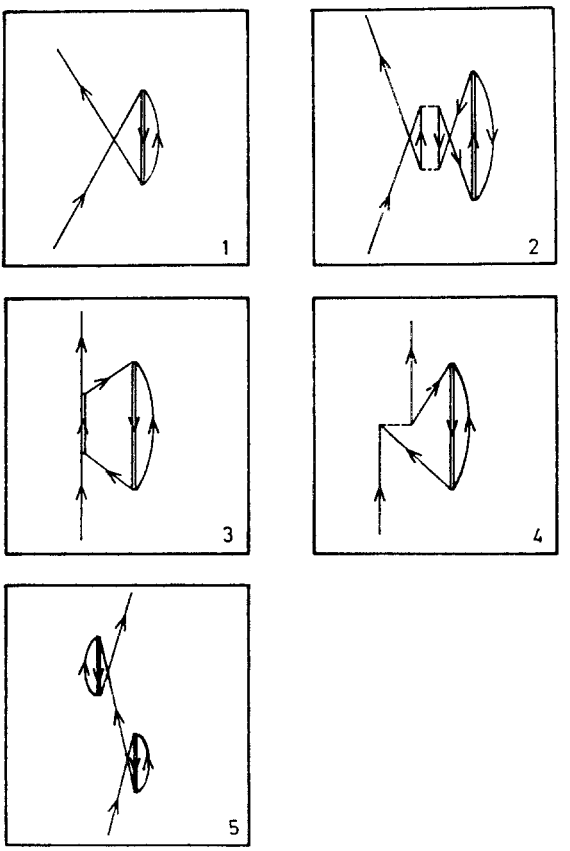

Fig 4 Diagrams contributing to the energy of a one-particle state.

The sign of each vertex is obtained according to the rules stated in the captions of figs. 1 and 2 and is given explicitly in fig. 7. Thus, four diagrams of the first row and the last diagram of the second row have two positive and two negative vertices. There is an additional minus sign due to the crossing between the two fermion lines In the three first diagrams of the second row, there are three negative and one positive vertices However, they yield contributions of the same sign as the previous

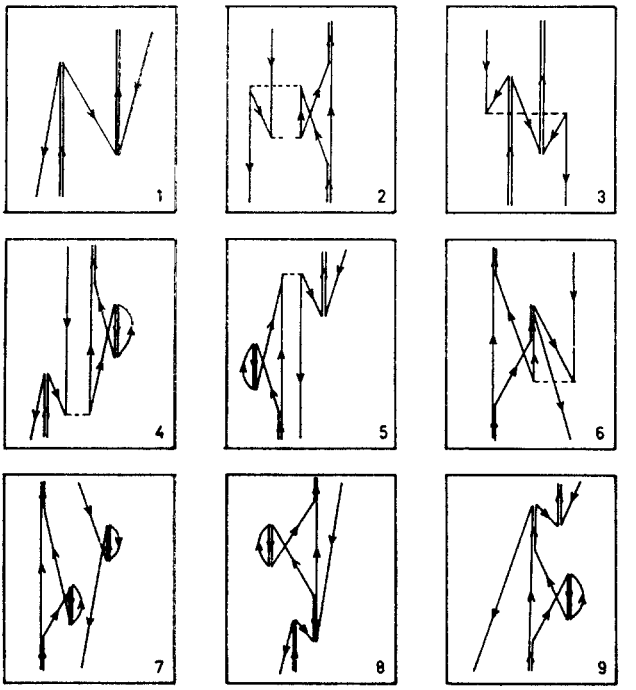

Fig 5 Diagrams contributing to the energy of the particle-phonon state

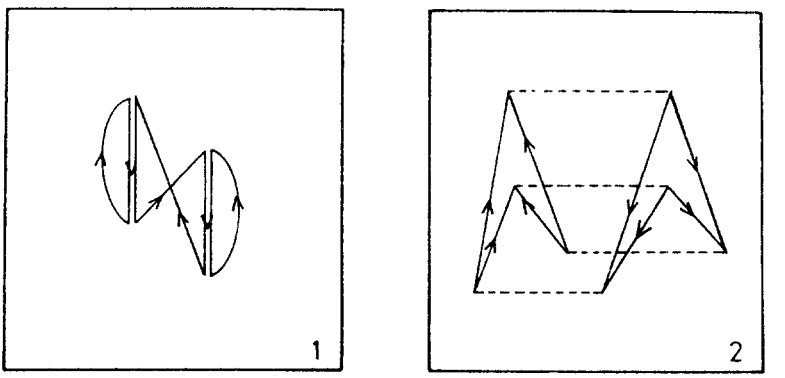

Fig. 6. Diagrams contributing to the energy of the ground state.

five, since there are no fermion crossings. Moreover, the product of the three denominators is negative, and thus all eight diagrams give a positive contribution.

The energy differences between initial and intermediate states are explicitly written in fig. 7. The energy of the initial state is denoted by E. Thus, the summed contribu-

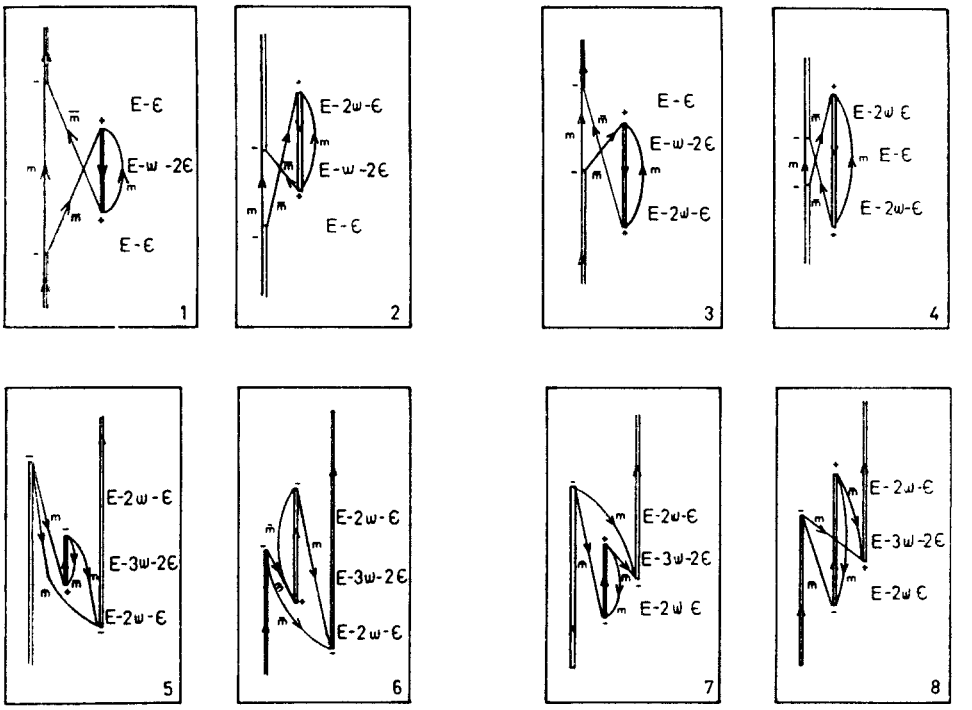

Fig 7 The time permutations corresponding to diagram 3.1. The sign of each vertex is explicitly indicated

tions of the eight diagrams in fig. 7 is

$$-\Lambda^4 2\Omega\left(\frac{1}{(E-\varepsilon)^2(E-\omega-2\varepsilon)}+\frac{2}{(E-\varepsilon)(E-\omega-2\varepsilon)(E-2\omega-\varepsilon)}\right.$$
$$\left.+\frac{1}{(E-\omega-2\varepsilon)(E-2\omega-\varepsilon)^2}+\frac{4}{(E-2\omega-\varepsilon)^2(E-3\omega-2\varepsilon)}\right)$$
$$=\frac{-\Lambda^4 8\Omega}{(E-\varepsilon-2\omega)^2}\left(\frac{(E-\varepsilon-\omega)^2}{(E-\omega-2\varepsilon)(E-\varepsilon)^2}+\frac{1}{(E-2\varepsilon-3\omega)}\right). \quad (2.25)$$

If we replace E by the unperturbed value ω, the contribution of the diagrams of fig 7 is

$$E^{(1)}(\mathbf{P})-E^{(1)}(\text{g.s})=\Lambda^4 4\Omega\left(\frac{\varepsilon}{(\varepsilon^2-\omega^2)^2}+\frac{1}{(\varepsilon+\omega)^3}\right). \quad (2.26)$$

Using (2.17) and (2 22) in (2.26) we obtain

$$E^{(1)}(\mathbf{P})-E^{(1)}(\text{g.s.})=\frac{x^4\varepsilon}{4\Omega(1-x)}\left(\frac{1}{x^2}+\frac{1}{(1+\sqrt{1-x})^3}\right)=\frac{x^2\varepsilon}{4\Omega}(1+x+\tfrac{9}{8}x^2+\ldots). \quad (2\,27)$$

Similarly, the other cases (cf. figs 4, 5 and 6) yield,

$$E^{(1)}(\mathbf{F})-E^{(1)}(\mathrm{g\,s}) = \frac{\Lambda^2}{\varepsilon+\omega} = \frac{x^2\varepsilon}{8\Omega}(1+\tfrac{3}{4}x+\tfrac{5}{8}x^2+\ldots), \tag{2.28}$$

$$E^{(1)}(\mathbf{1})-E^{(1)}(\mathbf{F})-E^{(1)}(\mathbf{P}) = \frac{\Lambda^2}{\varepsilon+\omega} = \frac{x^2\varepsilon}{8\Omega}(1+\tfrac{3}{4}x+\tfrac{5}{8}x^2+\ldots), \tag{2.29}$$

$$E^{(1)}(\mathrm{g\,s}) = \frac{\Lambda^4 4\Omega}{(\varepsilon+\omega)^3} = \frac{x^4\varepsilon}{32\Omega}+\ldots \tag{2.30}$$

To obtain the expansions (2.27)–(2.30), we utilized the series for ω in (2.22). In all cases (2.27)–(2.30), a single graph gives all powers of x and a single power of Ω^{-1}. We verify that the $a_{n,m=1}$ coefficients in (2.27)–(2.30) reproduce those obtained in the fermion calculation for $n \leqq 4$ (table 1).

The corrections of order Ω^{-2} are given by the remaining graphs of figs. 3, 4, 5 and 6. Only those graphs contributing with powers of x with $n \leqq 4$ are given in figs. 3, 4 and 6 and with $n \leqq 3$ in fig. 5. The last diagram in figs. 3 and 4 shows the initial state as intermediate state In this case the contributions to the coefficients $a_{n,m}$ listed in table 2 correspond to the time permutations yielding BW diagrams.

The renormalization diagrams corresponding to the time permutations of graphs 3.12, are obtained from the eight diagrams of fig. 7. Since we are calculating contributions of order Ω^{-2}, and the factor $\Lambda^4\Omega$ of these diagrams in (2.25) is already

TABLE 2

The values of the coefficients $a_{n,2}$ corresponding to the diagrams of figs. 3, 4, 5 and 6 (in units of $\frac{1}{128}$)

Graph	$E(\mathbf{P})-E(\mathrm{g\,s.})$		$E(\mathbf{F})-E(\mathrm{g\,s.})$		$E(\mathbf{1})-E(\mathbf{P})-E(\mathbf{F})$		$E(\mathrm{g.s.})$		$\partial W(E)/\partial E$	
	a_{32}	a_{42}	a_{32}	a_{42}	a_{22}	a_{32}	a_{32}	a_{42}	a_{22}	a_{32}
2	−8	−14		−4	−32	− 8		−2	−48	−48
3	−8	−12		−3		− 4			−48	−56
4		− 6	−4	−4		− 8				−24
5		− 4		−2		− 8				−16
6	−8	− 8				−32			−32	−32
7	−8	− 8							−32	−32
8		− 8				8				−32
9		− 8				8				−16
10		− 4								−16
11	−16	−24							−128	−144
12		− 4								−32
Renor.	32	52		1					192	256
Sum	−16	−48	−4	−12	−32	−44	0	−2	−96	−192

The contributions to $\partial W(E)/\partial E$ of fig 3 are also given in the same units.

of order Ω^{-1}, we are interested in the value of the bracket on the right-hand side of (2.25) up to order Ω^{-1}. This is obtained replacing E in the energy denominators by the sum of (2.22) and (2.27), and expanding to first order in Ω^{-1}. The result is

$$E^{(2)}(\mathbf{P})-E^{(2)}(\text{g.s}) = \frac{A^4 4}{\varepsilon^3 x}\left(1+\frac{(\varepsilon-\omega)^2}{\varepsilon(\varepsilon+\omega)}\right)\left(1-\tfrac{3}{2}(1-\tfrac{1}{2}x)\frac{(\varepsilon-\omega)^2}{\varepsilon\omega x}\right)$$
$$= \frac{\varepsilon x^3}{4\Omega^2}+\frac{13}{32}\frac{\varepsilon x^4}{\Omega^2}+\ldots. \tag{2.31}$$

We proceed similarly in order to evaluate the graphs of figs. 4.5, 5.8 and 5.9. The resulting contributions are given in the row labelled Renor. of table 2 (renormalization diagrams). In the three cases, they have opposite signs to the contributions of BW diagrams listed in the same table. There are no renormalization contributions in the case of the ground state, since they would imply unlinked graphs.

2.2.3 Calculation of matrix elements using the field Hamiltonian According to ref. [2]) we have to include both fermion and phonon terms in the field calculation of two-body transfer processes. To a fermion operator $\mathscr{P}^+$ creating two particles, there corresponds a field operator $\mathscr{P}^+_{\mathrm{f}}$,

$$\mathscr{P}^+ = \sum_{m>m'}(m\bar{1}, m'\bar{1}|\mathscr{P}^+|\mathrm{v})c^+_{m\bar{1}}c^+_{m'\bar{1}}+\sum_{m>m'}(m1, m'1|\mathscr{P}^+|\mathrm{v})c^+_{m1}c^+_{m'1},$$
$$\mathscr{P}^+_{\mathrm{f}} = \langle\psi_1|\mathscr{P}^+|\psi\rangle\Gamma^+_1+\langle\psi|\mathscr{P}^+|\psi_{\bar{1}}\rangle\Gamma_{\bar{1}}+\mathscr{P}^+. \tag{2.32}$$

Here $|m\sigma, m'\sigma\rangle$ denotes the (antisymmetrized) two-particle states. The RPA matrix elements of (2.32) are

$$\langle\psi_1|\mathscr{P}^+|\psi\rangle = \sum_{\substack{m>m'\\ \sigma}}(m\sigma, m'\sigma|\mathscr{P}^+|\mathrm{v})\langle\psi_1|c^+_{m\sigma}c^+_{m'\sigma}|\psi\rangle = \sum_{\substack{m>0\\ \sigma}}(m\sigma;\bar{m}\sigma|\mathscr{P}^+|\mathrm{v})$$
$$\times\langle\psi_1|c^+_{m\sigma}c^+_{\bar{m}\sigma}|\psi\rangle, \tag{2.33}$$

$$\langle\psi|\mathscr{P}^+|\psi_{\bar{1}}\rangle = \sum_{\substack{m>m\\ \sigma}}(m\sigma; m'\sigma|\mathscr{P}^+|\mathrm{v})\langle\psi|c^+_{m\sigma}c^+_{m'\sigma}|\psi_{\bar{1}}\rangle$$
$$= \sum_{\substack{m>0\\ \sigma}}(m\sigma;\bar{m}\sigma|\mathscr{P}^+|\mathrm{v})\langle\psi|c^+_{m\sigma}c^+_{\bar{m}\sigma}|\psi_{\bar{1}}\rangle. \tag{2.34}$$

Let us consider the two creation operators A^+_1 and $A^+_{\bar{1}}$. In these cases

$$(m\sigma; m'\sigma'|A^+_1|\mathrm{v}) = \delta_{\sigma,1}\delta_{m',\bar{m}}\delta_{\sigma,\sigma'}m/|m|,$$
$$(m\sigma; m'\sigma'|A_{\bar{1}}|\mathrm{v}) = \delta_{\sigma,\bar{1}}\delta_{m',\bar{m}}\delta_{\sigma,\sigma'}m/|m| \tag{2.35}$$

Using (2.32)-(2.35) we obtain

$$(A^+_1)_{\mathrm{f}} = A^+_1+\langle\psi_1|A^+_1|\psi\rangle\Gamma^+_1+\langle\psi|A^+_1|\psi_{\bar{1}}\rangle\Gamma_{\bar{1}} = A^+_1+\Omega(\lambda\Gamma^+_1+\mu\Gamma_{\bar{1}}), \tag{2.36}$$
$$(A_{\bar{1}})_{\mathrm{f}} = A_{\bar{1}}+\langle\psi_1|A_{\bar{1}}|\psi\rangle\Gamma^+_1+\langle\psi|A_{\bar{1}}|\psi_{\bar{1}}\rangle\Gamma_{\bar{1}} = A_{\bar{1}}+\Omega(\mu\Gamma^+_1+\lambda\Gamma_{\bar{1}}), \tag{2.37}$$

where the coefficients λ and μ are given in (2.14).

The operator (2.36) corresponds to the creation of two particles in the level above the Fermi level, while the operator (2.37) creates two particles in the level below.

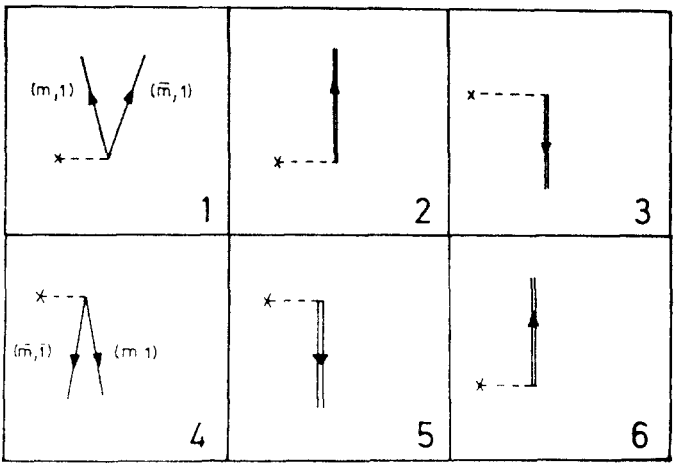

Fig 8 The vertices corresponding to the transfer operators $A_1{}^+$ (vertices 1, 2, 3) and $A_{\bar{1}}$ (vertices 3, 4, 5)

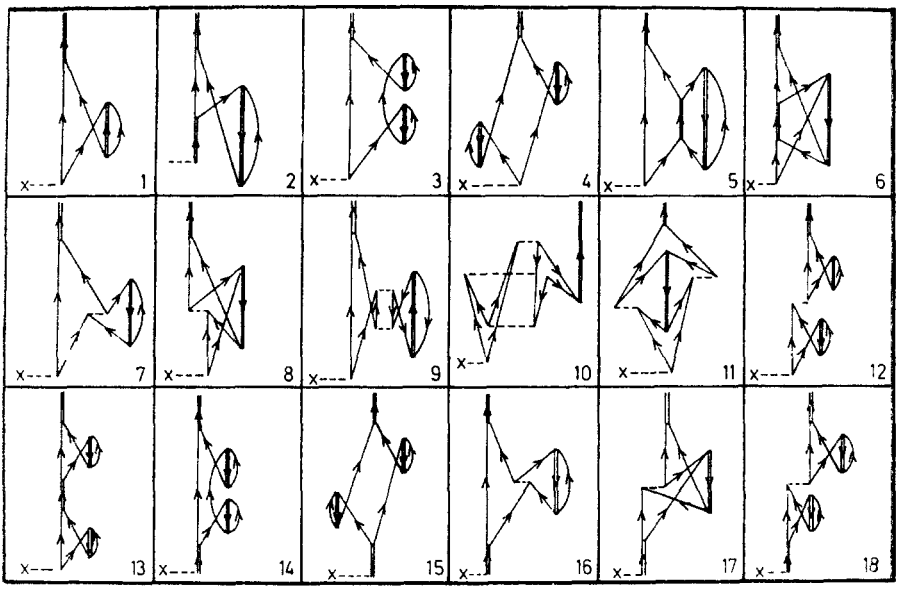

Fig 9 Diagrams contributing to the two-body transfer processes

Application of (2.37) to the unperturbed ground state $|0\rangle$ gives non-vanishing contributions only because of the existence of RPA ground-state correlations (see subsect. 2.2.4). The first and second terms in (2.36) would be the only ones in a TDA calculation [3]). There are three vertices for each operator A_1^+, $A_{\bar{1}}$ (fig. 8). Note that each pair of vertices (8.2, 8.6) and (8.3, 8.5) have the same graphical representation. Their value depends on whether we are calculating matrix elements corresponding to (2.36) or (2.37).

According to appendix B of ref. [3]), a matrix element of an operator T is given by the product of the effective matrix element $\langle \mathbf{P}|T|\text{g.s.}\rangle_e$ (which depends on the operator T itself) times the normalization of the initial and final states.

To leading order, the factor $\langle \mathbf{P}|T|\text{g.s.}\rangle_e$, corresponding to the transfer operators (2.36) and (2.37), is given by the value of the vertices 8 2 and 8 6, respectively,

$$\langle \mathbf{P}|A_1^+|\text{g.s.}\rangle_e^{(0)} = \tfrac{1}{2}(\varepsilon+\omega)(\Omega/\varepsilon\omega)^{\frac{1}{4}} = \Omega^{\frac{1}{4}}(1+\tfrac{1}{32}x^2+\tfrac{1}{32}x^3+\ldots), \tag{2.38}$$

$$\langle \mathbf{P}|A_{\bar{1}}|\text{g.s.}\rangle_e^{(0)} = \tfrac{1}{2}(\varepsilon-\omega)(\Omega/\varepsilon\omega)^{\frac{1}{4}} = \Omega^{\frac{1}{4}}(\tfrac{1}{4}x+\tfrac{1}{8}x^2+\tfrac{11}{128}x^3+\ldots) \tag{2.39}$$

In both cases, there are two different diagrams which yield contributions of order Ω^{-1} (with respect to the main term of order $\Omega^{\frac{1}{4}}$) The value corresponding to fig. 9.1 is

$$\langle \mathbf{P}|A_1^+|\text{g.s.}\rangle_e^{(1)} = -\tfrac{1}{2}x\Omega^{-\frac{1}{4}}(1+\tfrac{3}{4}x+\tfrac{21}{32}x^2+\ldots), \tag{2.40}$$

$$\langle \mathbf{P}|A_{\bar{1}}|\text{g.s.}\rangle_e^{(1)} = -\tfrac{1}{16}x^3\Omega^{-\frac{1}{4}}(1+\ldots). \tag{2.41}$$

Only those time permutations of fig. 9.1 in which the vertex 8.1 is present, contribute to (2.40). Only those in which 8.3 appears, contribute to (2 41).

The diagram 9 2 yields the following values

$$\langle \mathbf{P}|A_1^+|\text{g s.}\rangle_e^{(1)} = \tfrac{1}{16}x^3\Omega^{-\frac{1}{4}}(1+\ldots), \tag{2.42}$$

$$\langle \mathbf{P}|A_{\bar{1}}|\text{g s.}\rangle_e^{(1)} = -\tfrac{1}{8}x^2\Omega^{-\frac{1}{4}}(1+\tfrac{3}{2}x+\ldots). \tag{2.43}$$

The diagrams 9.3–9.18 contribute to the order Ω^{-2}. Table 3 lists the corresponding values for $n \leqq 3$. Only those time permutations of figs 9 14–9.18 representing BW diagrams are included.

TABLE 3

The contributions of order Ω^{-2} of the diagrams in fig 9 to the matrix elements of the transfer operators $A_1{}^+$ and $A_{\bar{1}}$ (in units of $\frac{1}{128}$)

Graph	$\langle \mathbf{P}\|A_1{}^+\|\text{g.s.}\rangle_e^{(2)}$		$\langle \mathbf{P}\|A_{\bar{1}}\|\text{g s}\rangle_e^{(2)}$
	a_{22}	a_{32}	a_{32}
3	16	24	
4	16	20	
5		12	
6		8	
7	16	12	
8	16	12	
9		16	
10		8	8
11		8	
12	32	40	
13		8	
14			4
15			4
16			4
17			4
18			8
Sum	96	168	32

Another contribution to the order Ω^{-2} is obtained by replacing the unperturbed energy of the final state by the expansion of the exact energy up to first order, in the energy denominators corresponding to the graphs 9.1 and 9.2 If the corresponding expressions are again expanded in powers of Ω^{-1}, graph 9.1 yields for the second-order contributions

$$\langle \mathbf{P}|A_1^+|\text{g s.}\rangle_e^{(2)} = -\tfrac{1}{2}x^2\Omega^{-\frac{1}{2}}(1+\tfrac{11}{8}x+\ \ldots\ ), \tag{2.44}$$

$$\langle \mathbf{P}|A_{\bar{1}}|\text{g.s.}\rangle_e^{(2)} = \mathrm{O}(x^4) \tag{2.45}$$

Similarly, we obtain for the case of diagram 9.2,

$$\langle \mathbf{P}|A_1^+|\text{g s}\rangle_e^{(2)} = (\mathrm{O}(x^4), \tag{2.46}$$

$$\langle \mathbf{P}|A_{\bar{1}}|\text{g.s}\rangle_e^{(2)} = -\tfrac{1}{8}x^3\Omega^{-\frac{3}{2}}(1+\quad) \tag{2.47}$$

Both the perturbed energies of the initial and final states must be used in the energy denominators However in (2.44)–(2.47) only the expansion for the energy of the final state has been used, while the unperturbed energy is used for the initial state This is because if the initial (or final) state is the vacuum state, any renormalization diagram (in which the vacuum is an intermediate state) is an unlinked diagram and thus must be disregarded

The effective matrix elements $\langle \mathbf{P}|A_1^+|\text{g s}\rangle_e$ and $\langle \mathbf{P}|A_{\bar{1}}|\text{g s.}\rangle_e$ (up to the order Ω^{-2}) are the summation of the contributions (2.38)–(2.47) plus those of table 3·

$$\langle \mathbf{P}|A_1^+|\text{g s}\rangle_e = \Omega^{\frac{1}{2}}\left(1+\tfrac{1}{3\,2}x^2+\tfrac{1}{3\,2}x^3-\frac{x}{2\Omega}-\frac{3x^2}{8\Omega}-\frac{25x^3}{64\Omega}+\frac{x^2}{4\Omega^2}+\frac{5x^3}{8\Omega^2}\right.$$
$$\left.+\mathrm{O}(x^4,\Omega^{-3})\right), \tag{2.48}$$

$$\langle \mathbf{P}|A_{\bar{1}}|\text{g.s.}\rangle_e = \Omega^{\frac{1}{2}}\left(\tfrac{1}{4}x+\tfrac{1}{8}x^2+\tfrac{11}{128}x^3-\frac{x^2}{8\Omega}+\frac{x^3}{4\Omega}+\frac{x^3}{8\Omega^2}+\mathrm{O}(x^4,\Omega^{-3})\right). \tag{2.49}$$

In order to obtain the matrix elements of the operators A_1^+, $A_{\bar{1}}$, we multiply (2 48) and (2 49) by the amplitudes of the initial and final states. According to appendix B of ref. [3]), the square of the amplitude of an unperturbed state is given by the same diagrammatic expansion as the energy of this state. The difference lies in the calculation of the denominators, since there is now a partial differentiation which introduces an additional energy difference.

Let us calculate in detail the contribution from the diagram 7.1 to the square root of the amplitude of the "bare" phonon state in the "dressed" state $|\mathbf{P}\rangle$. Only the time permutation given explicitly in the diagram is considered. In this case,

$$\frac{\partial W(E)}{\partial E} = \frac{-A^4 2\Omega}{(E-\varepsilon)^2(E-2\varepsilon-\omega)}\left(\frac{2}{E-\varepsilon}+\frac{1}{E-2\varepsilon-\omega}\right). \tag{2.50}$$

Introducing the first two terms in the expansion of E [i.e., $\omega+E^{(1)}$], we obtain the partial derivative (2 50) up to $O(\Omega^{-2})$,

$$\frac{\partial W(E)}{\partial E} = \frac{-\Lambda^4\Omega}{(\omega-\varepsilon)^2\varepsilon}\left(\frac{2}{\omega-\varepsilon}-\frac{1}{2\varepsilon}\right) - 2\Lambda^4 E^{(1)}\Omega\left(\frac{4}{(\omega-\varepsilon)^2}-\frac{1}{2\varepsilon^2}+\frac{1}{2\varepsilon(\omega-\varepsilon)}\right) + O(\Omega^{-3})$$

$$= \frac{x}{\Omega}+\frac{3x^2}{8\Omega}+\frac{5x^3}{16\Omega}+\frac{3x^2}{2\Omega^2}+\frac{7x^3}{4\Omega^2}+O(\Omega^{-3}, x^4). \tag{2.51}$$

Similarly we obtain the contributions of all diagrams of fig. 3 (table 2). The total value is

$$\frac{\partial W(E)}{\partial E} = \frac{x}{\Omega}+\frac{5x^2}{8\Omega}+\frac{5x^3}{8\Omega}-\frac{3x^2}{4\Omega^2}-\frac{3x^3}{2\Omega^2}+O(\Omega^{-3}, x^4). \tag{2 52}$$

The amplitude of the unperturbed phonon state in the final wave functions is

$$\left(1-\frac{\partial W(E)}{\partial E}\right)^{-\frac{1}{2}} = 1+\frac{x}{2\Omega}+\frac{5x^2}{16\Omega}+\frac{5x^3}{16\Omega}-\frac{9x^3}{32\Omega^2}+O(\Omega^{-3}, x^4). \tag{2.53}$$

The amplitude of the initial state is taken to be unity again because any difference with unity corresponds to unlinked diagrams for the vacuum state.

The product of (2 48) or (2 49) with (2 53) yields the coefficients $a_{n,m}$ listed in table 1, for the matrix elements $\langle \mathbf{P}|A_1^+|0\rangle$ and $\langle \mathbf{P}|A_{\bar{1}}|0\rangle$, respectively.

2 2.4 Interpretation of the diagrams We center the discussion on the nature of the vacuum state $|0\rangle$.

Within the field treatment, the vacuum state is the real vacuum both for particles and phonons.

$$c^+_{m\bar{1}}|0\rangle = c_{m1}|0\rangle = 0, \tag{2.54}$$

$$\Gamma_n|0\rangle = 0. \tag{2.55}$$

We also note that the only second-order diagrams 10.1 and 10.2 do not exist, since they contain bubbles Yet we know that the closed shell state [where (2 54) is valid] has first-order admixtures of two-particle, two-hole states. Therefore, the vacuum itself must contain all the ground-state RPA correlations, which agrees with (2 55) but is in contradiction to (2.54). This is further confirmed by the expression for the unperturbed energy of the vacuum state [eq. (2 24)] The graphical field treatment corrects this discrepancy in succesive orders of perturbation as follows:

In a Feynman diagrammatic expansion of the residual nuclear interaction, intermediate states may violate the Pauli principle However, for a given diagram in which two fermion lines are simultaneously in the same single-particle state, there is another diagram in which the corresponding end-points are interchanged This second diagram cancels the first one. For instance, in fig. 10.3, one of the possible intermediate states has $(m, 1) = (m_0, 1)$ This intermediate state cannot exist in the presence of an odd nucleon in the single-particle state $(m_0, 1)$. There is another

diagram (fig 10 4) in which the two fermion lines (m, 1, m_0, 1) are exchanged. The crossing of these two lines introduces a minus sign which cancels the component $m = m_0$ of the diagram 10 3, which violates the Pauli principle

The diagrams 10 3 and 10 4 are members of a subset of graphs which are replaced by diagram 10 5 and 10.6, respectively, within the field treatment of the residual interaction The cancellation of the spurious component also exists here (since we obtain the correct final results). The effect of the process represented in fig. 10 6 amounts to subtracting a component which should not be present in the initial state (fig. 10.5). Note that the fermion diagram 10.3 is included (among others) in 10.5, since the vacuum state used in graph 10.3 is the Hartree-Fock vacuum $|HF\rangle$, while the vacuum state corresponding to fig. 10 5 is the field ground state $|0\rangle$.

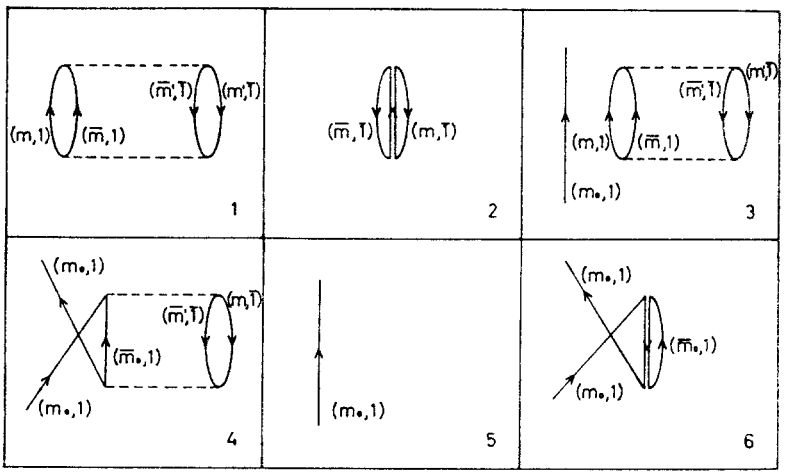

Fig 10 Diagrams illustrating the interpretation of the vacuum state $|0\rangle$ in the field treatment

3. The monopole particle-hole force in the two-level model

3 1 FERMION CALCULATION

Due to the presence of scattering terms in the monopole interaction, the initial Hamiltonian (3.1) does not satisfy the Hartree-Fock minimization conditions. Consequently, a transformation between single-particle states is carried out in the first part of this subsection. One obtains the new Hamiltonian (3.14), which may be treated within the field diagrammatic expansion.

In the second part of this subsection, a conventional perturbation calculation of (3.14) is outlined for various physical magnitudes.

The initial Hamiltonian is again divided in two parts,

$$H = H_{s.p.} + H_q, \tag{3.1}$$

$$H_{s\,p} = \tfrac{1}{2}\varepsilon_0(N_{1,0} + N_{\bar{1},0}), \tag{3.2}$$

$$H_q = -\tfrac{1}{2}V_0 Q^2, \tag{3.3}$$

$$Q = A_0^+ + A_0 + q_{1,0} N_{1,0} - q_{\bar{1},0} N_{\bar{1},0}, \tag{3.4}$$

where

$$N_{1,0} = \sum_m b_{m1}^+ b_{m1}, \qquad N_{\bar{1},0} = \sum_m b_{m\bar{1}} b_{m\bar{1}}^+, \qquad A_0^+ = \sum_m b_{m1}^+ b_{m\bar{1}} \tag{3.5}$$

Here, $b_{m\sigma}^+$ is the particle creation operator and $q_{1,0}$ ($q_{\bar{1},0}$) are the single-particle (single-hole) monopole moments The opposite signs in front of the last two terms in (3.4) reflects the opposite signs between the static multipole moments corresponding to particles and holes.

The Hamiltonian (3.1) has non-vanishing matrix elements between the closed shell state and particle-hole states. Therefore, one must perform a Hartree-Fock transformation between single-particle states

$$c_{m1} = z b_{m1} - y b_{m\bar{1}}, \qquad c_{m\bar{1}} = y b_{m1} + z b_{m\bar{1}}, \qquad z^2 + y^2 = 1. \tag{3.6}$$

Using the inverse transformation to (3 6), we express the monopole operator (3.4) in terms of the new creation and annihilation operators $c_{m\sigma}^+$ and $c_{m\sigma}$. The corresponding expression is analogous to (3.4),

$$Q = q(A^+ + A + q_1 N_1 - q_{\bar{1}} N_{\bar{1}} + q_0), \tag{3.4'}$$

where A^+ and N_σ are defined by analogy with (3.5) and (2 5),

$$N_1 = \sum_m c_{m1}^+ c_{m1}, \qquad N_{\bar{1}} = \sum_m c_{m\bar{1}} c_{m\bar{1}}^+, \qquad A^+ = \sum_m c_{m1}^+ c_{m\bar{1}}, \tag{3.5'}$$

and the constants q_a have the values

$$\begin{aligned} q_1 &= (q_{1,0} z^2 + q_{\bar{1},0} y^2 - 2yz)/q, \qquad & q_{\bar{1}} &= (q_{\bar{1},0} z^2 + q_{1,0} y^2 + 2yz)/q, \\ q_0 &= 2\Omega y(2z + y(q_{1,0} - q_{\bar{1},0}))/q, \qquad & q &= z^2 - y^2 + yz(q_{1,0} - q_{\bar{1},0}) \end{aligned} \tag{3.7}$$

Inserting (3.4′) in (3.3), the monopole interaction can be written as

$$\begin{aligned} H_q &= -\tfrac{1}{2}V(A^+ + A + q_1 N_1 - q_{\bar{1}} N_{\bar{1}} + q_0)^2 \\ &= -\tfrac{1}{2}V((A^+)^2 + A^2) \\ &\quad - V(A^+(q_1 N_1 - q_{\bar{1}} N_{\bar{1}}) + (q_1 N_1 - q_{\bar{1}} N_{\bar{1}})A + \tfrac{1}{2}(A^+ + A)(q_1 - q_{\bar{1}} + 2q_0)) \\ &\quad - V(A^+ A + \tfrac{1}{2}(q_1 N_1 - q_{\bar{1}} N_{\bar{1}} + q_0)^2 + \Omega - \tfrac{1}{2}N_1 - \tfrac{1}{2}N_{\bar{1}}), \end{aligned} \tag{3.8}$$

where

$$V = V_0 q^2. \tag{3.9}$$

TABLE

The fermion calculation of the coefficients $a_{n,m}$ for two energies and for a

	n				$(q_1+q_{\bar{1}})^2$		$(q_1-q_{\bar{1}})^2$		$q_1{}^2-q_{\bar{1}}{}^2$	
		a_{n0}	a_{n1}	a_{n2}	a_{n1}	a_{n2}	a_{n1}	a_{n2}	a_{n1}	a_{n2}
$E(S)-E(g\,s)$	0	128								
	1	−64			8		−8			
	2	−16	32	−12			−32	16		
	3	−8	32	−32	1	−2	−73	111		
$E(2)-E(S)-E(F)$	0									
	1		32				−16		−16	
	2		16	−20		4	−32	52	−32	40
	3		12	−38		11	−42	203	−42	142
$\langle S\|Q\|g\,s.\rangle$	0	128								
	1	32	−16							
	2	20	−24	7	−2	1	14	−7		

The single-particle term takes the form

$$H_{s\,p} = \varepsilon_0(yz(A^+ + A)+\tfrac{1}{2}(z^2-y^2)(N_1+N_{\bar{1}})+2\Omega y^2). \tag{3.10}$$

From eqs. (3.8) and (3 10) we obtain the Hartree-Fock condition concerning the vanishing of the matrix elements between the ground state and the particle-hole states

$$\varepsilon_0\, yz = \tfrac{1}{2}V(q_1-q_{\bar{1}}+2q_0). \tag{3 11}$$

Introducing (3.8) and (3 10) in (2.6), the Hartree-Fock energies ε_σ are

$$\begin{aligned} \varepsilon_1 &= \tfrac{1}{2}(\varepsilon_0(z^2-y^2)+V-Vq_1^2-2Vq_1 q_0), \\ \varepsilon_{\bar{1}} &= -\tfrac{1}{2}(\varepsilon_0(z^2-y^2)+V-Vq_{\bar{1}}^2+2Vq_{\bar{1}} q_0) \end{aligned} \tag{3.12}$$

Therefore, the particle-hole Hartree-Fock excitation energies ε are

$$\varepsilon = \varepsilon_1-\varepsilon_{\bar{1}} = \varepsilon_0(z^2-y^2)+V(1-\tfrac{1}{2}(q_1^2+q_{\bar{1}}^2)-q_0(q_1-q_{\bar{1}})). \tag{3.13}$$

It is convenient to transfer the Hartree-Fock contributions given in the second term of (3.13) from (3.8) to (3.10). Thus, we redistribute the terms in the total Hamiltonian (3.1) and obtain

$$H = H'_{s\,p}+H'_q+U,$$

$$H'_{s\,p} = \varepsilon_1 N_1-\varepsilon_{\bar{1}} N_{\bar{1}},$$

4

transition matrix element, in units of $\frac{1}{128}$ (monopole particle-hole interaction)

$\frac{(q_1-q_{\bar{1}})^4}{a_{n2}}$	$\frac{(q_1{}^2-q_{\bar{1}}{}^2)^2}{a_{n2}}$	$\frac{(q_1+q_{\bar{1}})^3(q_1-q_{\bar{1}})}{a_{n2}}$	$\frac{(q_1+q_{\bar{1}})(q_1-q_{\bar{1}})^3}{a_{n2}}$
−10	2		
−20	−4	2	−26

$$H'_q = -\tfrac{1}{2}V((A^+)^2+2A^+A+A^2)-V(A^+(q_1N_1-q_{\bar{1}}N_{\bar{1}})+(q_1N_1-q_{\bar{1}}N_{\bar{1}})A) \\ -\tfrac{1}{2}V((q_1N_1-q_{\bar{1}}N_{\bar{1}})^2-q_1^2N_1-q_{\bar{1}}^2N_{\bar{1}}), \quad (3\,14)$$

$$U = \varepsilon\Omega y^2 - V\Omega - \tfrac{1}{2}Vq_0^2.$$

The Hamiltonian (3.14) has a suitable form for application of the field formalism since the single-particle term contains all the Hartree-Fock contributions and H'_q satisfies the Hartree-Fock conditions for the state $|\mathrm{HF}\rangle$. The relation between the constants V, q_σ and the initial ones V_0, $q_{\sigma,0}$ and, more generally, the solutions of (3.11) are not relevant to our problem †. From now on, we operate with (3.14)

The non-vanishing matrix elements of H (3.14) are also constructed in appendix A, using again the quasispin formalism. The resultant matrices are diagonalized in perturbation theory. Each resultant energy (or matrix element) has different terms, corresponding to different combinations of q_1, $q_{\bar{1}}$. In addition, each term contains a factor of the form (1.1), where x is now defined as

$$x = 4V\Omega/\varepsilon. \quad (3.15)$$

The lower coefficients of these double series are listed in table 4. The labels

† The aim of sect. 3 is to treat a Hamiltonian which presents all the vertices of fig. 11 and which satisfies the HF conditions (such as (3 14)), independent of the derivation of this Hamiltonian.

(g.s.) and (S) denote the ground and first excited state of the closed shell system, while (2) denotes the first excited state of the odd system †.

3 2 NUCLEAR FIELD CALCULATION OF THE MONOPOLE INTERACTION

For the monopole interaction (3.14) we have the possibility to include only direct vertices 11.1 and 11 2 [eq. (3.16)] in the definition of the phonon, or to include both the direct and the exchange vertices 11.1, 11.2 and 11.5 [eq. (3.33)] In the first case, the construction of the phonon is simplified, but at the expense of having to consider more graphs than in the second case.

3 3 THE FIELD TREATMENT OF THE MONOPOLE INTERACTION

3.3.1. Inclusion of the direct component of the interaction in the construction of the phonon. The matrix element of the monopole interaction between non-antisymmetrized states can be written as

$$\begin{aligned}(m_1\sigma_1; m_2\sigma_2|H'_q|m'_1\sigma'_1; m'_2\sigma'_2) &= -(V/q^2)(m_1\sigma_1|Q|m'_1\sigma'_1)(m_2\sigma_2|Q|m'_2\sigma'_2),\\ (m\sigma|Q|m'\sigma') &= \delta_{mm'}(\delta_{\sigma-\sigma'}+\delta_{\sigma\sigma'}\sigma q_\sigma).\end{aligned} \tag{3.16a}$$

The direct and exchange matrix elements are separately represented in fig 11. The corresponding values are

$$\begin{aligned}
(m_3\,1; m_2\,\bar{1}|H'_q|m_4\,\bar{1}; m_1\,1) &= -V\delta_{m_1m_2}\delta_{m_3m_4} && \text{(fig. 11.1)},\\
(m_3\,\bar{1}, m_2\,\bar{1}|H'_q|m_4\,1, m_1\,1) &= -V\delta_{m_1m_2}\delta_{m_3m_4} && \text{(fig. 11.2)},\\
(m_2\,\bar{1}; m_3\,1|H'_q|m_1\,1; m_4\,1) &= -Vq_1\delta_{m_1m_2}\delta_{m_3m_4} && \text{(fig. 11 3)},\\
(m_2\,\bar{1}; m_3\,\bar{1}|H'_q|m_1\,1; m_4\,\bar{1}) &= Vq_{\bar{1}}\delta_{m_1m_2}\delta_{m_3m_4} && \text{(fig. 11.4)},\\
(m_2\,\bar{1}; m_3\,1|H'_q|m_4\,\bar{1}; m_1\,1) &= Vq_1q_{\bar{1}}\delta_{m_1m_3}\delta_{m_2m_4} && \text{(fig. 11.5)},\\
(m_2\,1; m_3\,1|H'_q|m_4\,1; m_1\,1) &= -Vq_1^2\delta_{m_1m_3}\delta_{m_2m_4} && \text{(fig. 11.6)},\\
(m_3\,\bar{1}; m_2\,\bar{1}|H'_q|m_1\,\bar{1}; m_4\,\bar{1}) &= -Vq_{\bar{1}}^2\delta_{m_1m_3}\delta_{m_2m_4} && \text{(fig. 11.7)}.
\end{aligned} \tag{3.16b}$$

The vertices of figs. 11 1 and 11.2 correspond to a separable interaction, for which the RPA solutions are easily obtained. Because of the symmetries of the problem, there is again a single collective frequency ω. As for the pairing case,

$$\omega = \varepsilon(1-x)^{\frac{1}{2}}, \tag{3 17}$$

where x is defined in (3.15). We also obtain the amplitudes

$$\begin{aligned}\langle\psi_1|c^+_{m1}\,c_{m'\bar{1}}|\psi\rangle &= \lambda\delta_{mm'} = \tfrac{1}{2}(\varepsilon+\omega)(2\varepsilon\omega\Omega)^{-\frac{1}{2}}\delta_{mm'},\\ \langle\psi_1|c^+_{m'\bar{1}}\,c_{m1}|\psi\rangle &= \mu\delta_{mm'} = \tfrac{1}{2}(\varepsilon-\omega)(2\varepsilon\omega\Omega)^{-\frac{1}{2}}\delta_{mm'},\end{aligned} \tag{3.18}$$

† (2) ≡ ($\uparrow$ §)

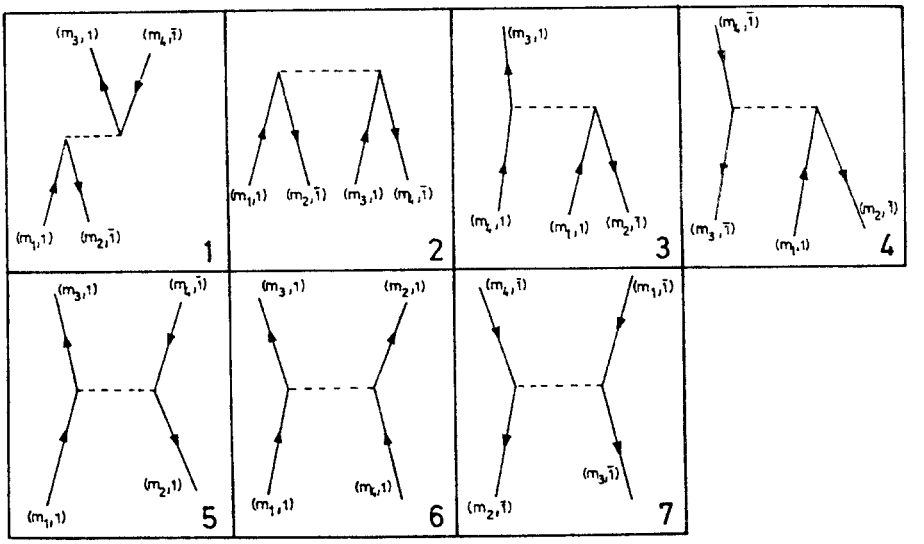

Fig. 11. The matrix element corresponding to the direct and exchange components of the monopole interaction. We use the convention that the particle-hole pair which approaches a vertex from the same side, has the particle always to the left. If the hole line appears to the left, a minus sign should be added.

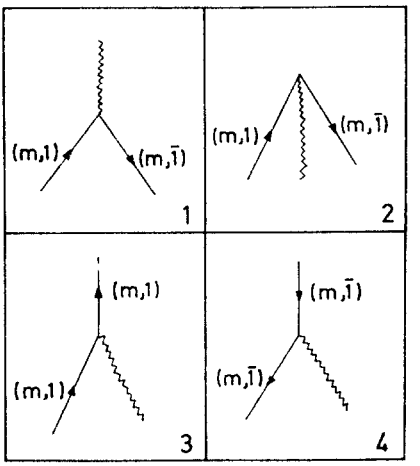

Fig. 12. The vertices corresponding to the particle-vibration interaction The fermion lines are ordered as in fig 11.

Here $|\psi_1\rangle$ is the RPA state with one phonon. We denote by Γ^+ the phonon creation operator. Thus, the pure boson term in the field Hamiltonian reads

$$H_b = \omega \Gamma^+ \Gamma. \tag{3 19}$$

The particle-vibration interaction vertices are given in ref. [2]).

$$
\begin{aligned}
\Lambda(m_1 1; m_2 \bar{1}) &= \langle 0|\Gamma H_{\mathrm{p\,v}}\, c^{+}_{m_1 1}\, c_{m_2 \bar{1}}|0\rangle \\
&= \sum_{m,m'} (m_1 1; m'\bar{1}|H'_q|m_2 \bar{1}; m1)\langle\psi_1|c^{+}_{m1}\, c_{m'\bar{1}}|\psi\rangle \\
&\quad + \sum_{m,m'} (m_1 1; m1|H'_q|m_2 \bar{1}; m'\bar{1})\langle\psi_1|c^{+}_{m'\bar{1}}\, c_{m1}|\psi\rangle \\
&= \delta_{m_1,m_2} \sum_{m} ((m_1 1; m\bar{1}|H'_q|m_1 \bar{1}, m1)\lambda + (m_1 1, m1|H'_q|m_1 \bar{1}, m\bar{1})\mu) \\
&= -\Lambda\delta_{m_1,m_2} \qquad \text{(fig. 12 1)}, \\
\Lambda(m_2 \bar{1}; m_1 1) &= \langle 0|H_{\mathrm{p\,v}}\, \Gamma^{+} c^{+}_{m_1 1}\, c_{m_2 \bar{1}}|0\rangle \\
&= \sum_{m,m'} ((m_2 \bar{1}; m'\bar{1}|H'_q|m_1 1, m1)\langle\psi_1|c^{+}_{m1}\, c_{m'1}|\psi\rangle \\
&\quad + (m_2 \bar{1}; m1|H'_q|m_1 1, m'\bar{1})\langle\psi_1|c^{+}_{m'\bar{1}}\, c_{m1}|\psi\rangle) \\
&= \delta_{m_1 m_2} \sum_{m} ((m_1 \bar{1}; m\bar{1}|H'_q|m_1 1; m1)\lambda + (m_1 \bar{1}, m1|H'_q|m_1 1, m\bar{1})\mu) \\
&= -\Lambda\delta_{m_1 m_2} \qquad \text{(fig. 12 2)}, \\
\Lambda(m_1 1, m_2 1) &= \langle 0|c_{m_1 1}\, H_{\mathrm{p\,v}}\, c^{+}_{m_2 1}\, \Gamma^{+}|0\rangle \\
&= \sum_{m,m'} ((m_1 1; m'\bar{1}|H'_q|m_2 1, m1)\langle\psi_1|c^{+}_{m1}\, c_{m'\bar{1}}|\psi\rangle \\
&\quad + (m_1 1; m1|H'_q|m_2 1; m'\bar{1})\langle\psi_1|c^{+}_{m'\bar{1}}\, c_{m1}|\psi\rangle \\
&= \delta_{m_1 m_2} \sum_{m} ((m_1 1; m\bar{1}|H'_q|m_1 1; m1)\lambda + (m_1 1; m1|H'_q|m_1 1; m\bar{1})\mu) \\
&= -\Lambda q_1 \delta_{m_1 m_2} \qquad \text{(fig. 12 3)}, \qquad (3\,20) \\
\Lambda(m_1 \bar{1}; m_2 \bar{1}) &= \langle 0|c^{+}_{m_2 \bar{1}}\, H_{\mathrm{p\,v}}\, c_{m_1 \bar{1}}\, \Gamma^{+}|0\rangle \\
&= \sum_{m,m'} ((m_1 \bar{1}, m'\bar{1}|H'_q|m_2 \bar{1}; m1)\langle\psi_1|c_{m1}\, c^{+}_{m'\bar{1}}|\psi\rangle \\
&\quad + (m_1 \bar{1}; m1|H'_q|m_2 \bar{1}, m'\bar{1})\langle\psi_1|c^{+}_{m'\bar{1}}\, c_{m1}|\psi\rangle) \\
&= \delta_{m_1 m_2} \sum_{m} ((m_1 \bar{1}; m\bar{1}|H'_q|m_1 \bar{1}, m1)\lambda + (m_1 \bar{1}, m1|H'_q|m_1 \bar{1}, m\bar{1})\mu) \\
&= \Lambda q_{\bar{1}}\, \delta_{m_1 m}, \qquad \text{(fig 12.4)}.
\end{aligned}
$$

Here,

$$\Lambda = V2\Omega(\lambda+\mu) = \tfrac{1}{2}x\varepsilon(\varepsilon/2\Omega\omega)^{\frac{1}{2}}. \qquad (3.21)$$

The four vertices (3.20) are represented in fig 12. Note that there are two more vertices here (the two scattering vertices) than for the pairing case (fig 2)

The particle-vibration interaction corresponding to fig 12 and eq. (3 20) is

$$H_{\mathrm{p\,v}} = -\Lambda(\Gamma^{+}+\Gamma)(A^{+}+A+q_1 N_1 - q_{\bar{1}} N_{\bar{1}}). \qquad (3.22)$$

The total field Hamiltonian is obtained from (3.14), (3.19) and (3.22)

$$H_f = H'_{sp} + H'_q + H_b + H_{pv} + U. \tag{3 23}$$

One must add to (3 23) the (diagrammatic) rule that no successive vertices as the ones appearing in figs 11 and 12 occur between the same pair of particle-hole lines

The zero-order excitation energy of the one-phonon state is given again by ω,

$$E^{(0)}(S) - E^{(0)}(g.s.) = \omega = (1 - \tfrac{1}{2}x - \tfrac{1}{8}x^2 - \tfrac{1}{16}x^3 - \ \ldots), \tag{3 24}$$

which agrees with the Ω^0 results of the fermion calculation (table 4)

The diagrams contributing to the order Ω^{-1} and Ω^{-2} are given in figs. 13 and 14 (respectively) for the one-phonon case The corresponding values are listed in tables 5 and 6. As usual, only the values originated from BW diagrams are given. Those Ω^{-2} contributions derived from renormalization diagrams are again obtained using the Ω^{-1} terms in the expansion of the exact energy in the denominators (as illustrated in detail for the pairing case). These contributions are given in the last to one row (labelled Renor) of table 6 All the values listed in tables 5 and 6 are of similar order of magnitude, which makes it difficult to select a subset of graphs of particular relevance. We also notice that partial summations are dangerous: for instance, if we exactly solve the equation for the energy in the Brillouin-Wigner perturbation expansion, we obtain renormalization contributions. These contributions are systematically of opposite sign as those arising from BW diagrams. In particular, in the case of table 6, they cancel most of the fourth-order contributions in $q_1, q_{\bar{1}}$.

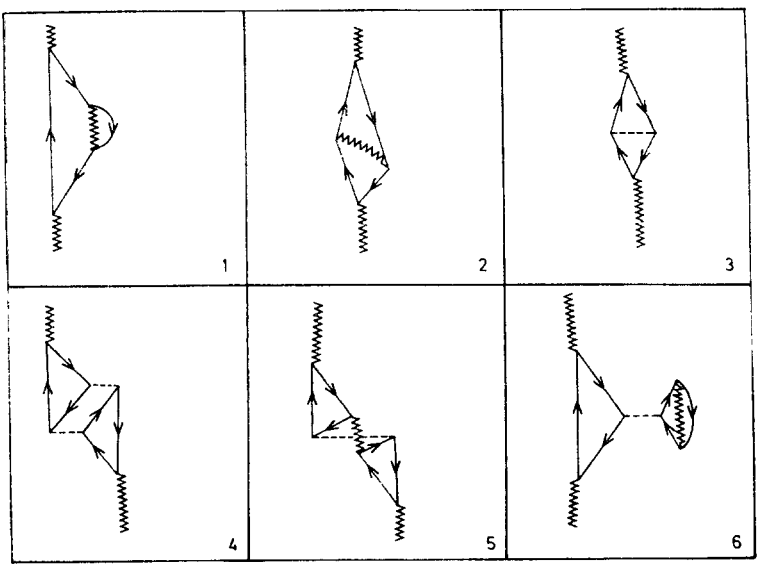

Fig 13 Diagrams corresponding to the order Ω^{-1} in the energy of the one-phonon state.

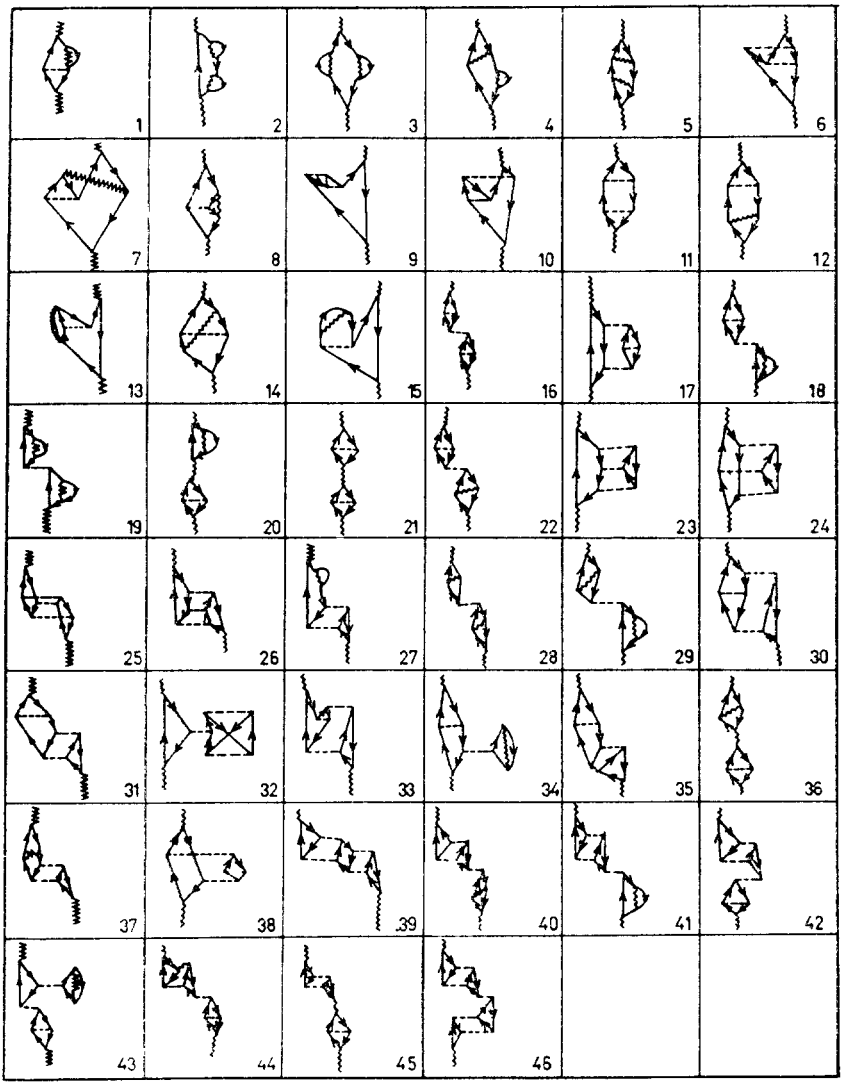

Fig 14 Diagrams corresponding to the order Ω^{-2} in the energy of the one-phonon state

The particle-phonon case is studied in appendix C

The large number of diagrams in figs 14 and 21, rules out the application of the field approach to physical situations in which powers higher than Ω^{-2} become necessary

Within the field treatment, the monopole operator Q_f corresponding to Q [eq.

TABLE 5

The contributions of the diagrams in fig. 13 to the coefficients $a_{n,1}$ (in units of $\frac{1}{128}$)

Graph			$(q_1+q_{\bar{1}})^2$			$(q_1-q_{\bar{1}})^2$		
	x^2/Ω	x^3/Ω	x/Ω	x^2/Ω	x^3/Ω	x/Ω	x^2/Ω	x^3/Ω
1	16	16		−8			−8	−16
2		8		8			−8	− 8
3	16	8	8		1	−8		− 1
4							−16	− 4
5								−34
6								−10
Sum	32	32	8	0	1	−8	−32	−73

(3.4′)] has both the fermion term (3.4′) plus a boson term Q_b,

$$Q_f = Q+Q_b, \tag{3 25}$$

$$Q_b = \langle\psi_1|Q|\psi\rangle\Gamma^+ + \langle\psi|Q|\psi_1\rangle\Gamma = q(\langle\psi_1|(A^+ + A)|\psi\rangle\Gamma^+ + \langle\psi|(A^+ + A)|\psi_1\rangle\Gamma)$$

$$= q2\Omega(\lambda+\mu)(\Gamma^+ + \Gamma) = q(2\Omega\varepsilon/\omega)^{\frac{1}{2}}(\Gamma^+ + \Gamma), \tag{3 26}$$

where use has been made of (3.18) Thus, the operator (3.25) has the vertices represented in fig. 15. As for the energy, the matrix elements of (3.25) have to be diagrammatically obtained. The graphs involving successive interactions between the same particle-hole lines have to be disregarded as usual.

We study, in particular, the matrix element of (3.25) between the ground and the first excited state for the closed shell system.

The zero-order contribution to the effective matrix element is given by the phonon vertex in eq. (3 26), namely

$$\langle \mathbf{S}|Q|\mathrm{g\ s}\rangle_e^{(0)} = q(2\Omega\varepsilon/\omega)^{\frac{1}{2}} = (2\Omega)^{\frac{1}{2}}q(1+\tfrac{1}{4}x+\tfrac{5}{32}x^2+\ .\ .). \tag{3 27}$$

The graphs of fig. 16 yield the first-order contributions to the effective matrix element. The corresponding values are listed in the columns labelled x^ν/Ω ($\nu = 0$, 1, 2) in table 7. The values that are given in rows 7–10 of these columns correspond to the possible time permutations of the graphs 16 7–16 10, involving only BW diagrams.

The columns labelled $x^n E^{(1)}/\Omega$ of table 7 yield the Ω^{-2} contributions of diagrams 16 when the exact energy $E(\mathbf{S})$ is approximated by the linear expression

$$E(\mathbf{S}) \approx \omega + E^{(1)}, \tag{3 28}$$

where $E^{(1)}$ is given in table 5, and the inverse of the denominators is expanded in powers of Ω^{-1} The energy of the initial (vacuum) state is always kept equal to zero,

TABLE 6

The contributions of the diagrams in fig 14 to the coefficients $a_{n,2}$ (in units of $\frac{1}{128}$)

Graph			$(q_1+q_{\bar{1}})^2$		$(q_1-q_{\bar{1}})^2$		$(q_1+q_{\bar{1}})^4$			$(q_1^2-q_{\bar{1}}^2)^2$			$(q_1-q_{\bar{1}})^4$		
	x^2	x^3	x^2	x^3	x^2	x^3	x	x^2	x^3	x	x^2	x^3	x	x^2	x^3
1		−4	−4	−3	4	11		2				2		−2	−2
2		−2		2		2			$-\frac{1}{2}$			−3			$-\frac{1}{2}$
3		−2		2		2			$-\frac{1}{2}$			1			$-\frac{1}{2}$
4				−4		4			2						−2
5									−1			2			−1
6			4	−3	4	1									
7				−8		8									
8				−5		7			$\frac{1}{2}$						$-\frac{1}{2}$
9	−8	−2	4	−4	4	4									
10		−4	−8	7	8	1									
11	−4	−2	−2	−1	2	1	−1	$\frac{1}{4}$		2	$-\frac{1}{2}$		−1	$\frac{1}{4}$	
12		−4		−1		5		−2			4	+1		−2	−1
13		−8		7		9									
14		−2		6		6			$-\frac{1}{2}$			1			$-\frac{1}{2}$
15		−2				4									
16		−4	−4		4		−1	$\frac{1}{2}$	$-\frac{1}{8}$	2	−1	$\frac{1}{4}$	−1	$\frac{1}{2}$	$-\frac{1}{8}$
17		−4		$\frac{5}{2}$		$\frac{5}{2}$			$\frac{1}{2}$						$-\frac{1}{2}$
18		−8	−4	2	4	6		2	−1			4		−2	−3
19		−4		4		4			−1			−2			−1
20				−1		1			$\frac{1}{2}$						$-\frac{1}{2}$
21				$-\frac{3}{2}$		$\frac{3}{2}$		$-\frac{1}{4}$	$-\frac{1}{8}$		$\frac{1}{2}$	$\frac{1}{4}$		$-\frac{1}{4}$	$-\frac{1}{8}$
22				−6		6		−2	1		4			−2	−1
23						7						−3			−1

24					5						3			−3
25		−4		4	4			1			2			−3
26				−4	4			−1			−2			−1
27					8						−4			−4
28								−1			2			−1
29				−4	4			2						−2
30					14						2			−2
31					10					4	$-\frac{3}{2}$		−4	$\frac{3}{2}$
32					5									
33					12									
34											$\frac{5}{2}$			$-\frac{5}{2}$
35											$\frac{17}{2}$			$-\frac{17}{2}$
36								$-\frac{1}{2}$			1			$-\frac{1}{2}$
37											4			−4
38				−2	2			$-\frac{1}{2}$			1			$-\frac{1}{2}$
39														−4
40											4			−4
41					8						−4			−4
42					8					4	−1		−4	1
43											$\frac{5}{2}$			$-\frac{5}{2}$
44											$\frac{17}{2}$			$-\frac{17}{2}$
45											1			−1
46														−4
Sum(p)	−12	−56	−14	−12	30	177	−2	0.5	−0.25	4	15	33	−2	−15.5	−72 75
Renor	0	24	14	10	−14	−66	2	−0.5	0.25	−4	−15	−31	2	15 5	62 75
Sum	−12	−32	0	−2	16	111	0	0	0	0	0	2	0	0	−10

The row labelled Sum(p) is the sum of the rows 1–46. The last row is the sum of the two previous ones Thus, it also includes the contributions from renormalization graphs, which are given in the row labelled Renor.

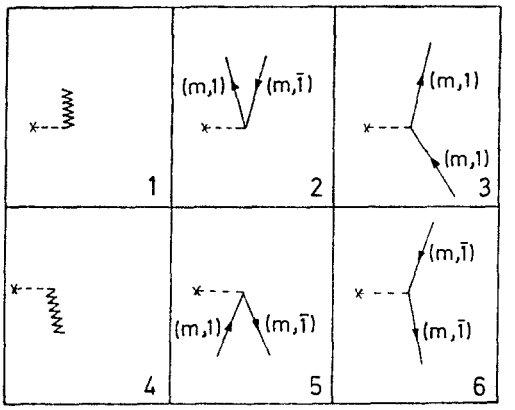

Fig 15 The vertices corresponding to the monopole operator Q

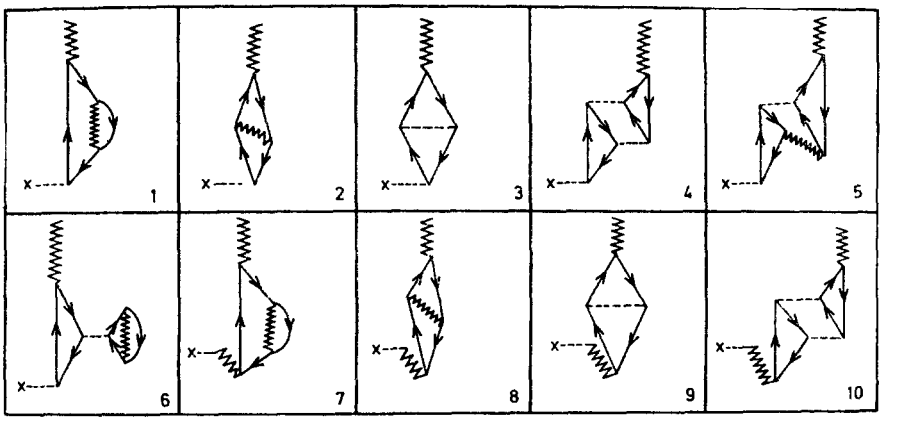

Fig 16 Diagrams contributing to the order Ω^{-1} in the matrix element of the operator Q corresponding to the transition between the ground state and the one-phonon state

since the corresponding renormalization diagrams are necessarily unlinked diagrams, and therefore can be disregarded.

Other second-order contributions to the effective matrix element are given by the time permutations of graphs 17 giving BW diagrams. The corresponding values are listed in table 8

The remaining contributions of order Ω^{-2} are given by the diagrams which may be obtained from those of fig. 14 if we substitute the initial or final phonon by the vertices 15 2 and 15.5 as indicated in fig. 18. Thus, the corresponding values are obtained by multiplying by $-q/\Lambda$ the results given in table 6 These last contri-

TABLE 7

Contributions of the diagrams of fig 16 to the matrix element of the operator Q between the ground state and the one-phonon state (in units of $\frac{1}{128}$)

Graph	$\varkappa/\Omega$	$\varkappa^2/\Omega$	$\frac{E^{(1)}}{\varepsilon\Omega}$	$\frac{E^{(1)}x}{\varepsilon\Omega}$	$(q_1+q_{\bar{1}})^2$						$(q_1-q_{\bar{1}})^2$					
					$1/\Omega$	$\varkappa/\Omega$	$\varkappa^2/\Omega$	$\frac{E^{(1)}}{\varepsilon x\Omega}$	$\frac{E^{(1)}}{\varepsilon\Omega}$	$\frac{E^{(1)}\varkappa}{\varepsilon\Omega}$	$1/\Omega$	$\varkappa/\Omega$	$\varkappa^2/\Omega$	$\frac{E^{(1)}}{\varepsilon x\Omega}$	$\frac{E^{(1)}}{\varepsilon\Omega}$	$\frac{E^{(1)}x}{\varepsilon\Omega}$
1	−32	−24	−128	−48		16	−4		64			16	28		64	64
2		−16		−32		−16	4		−64			16	12		64	32
3	−32	−8	−64	8	−16	4	$-\frac{1}{2}$	−64	32	2	16	−4	$\frac{1}{2}$	64	−32	−2
4												32			128	−48
5													20			80
6													68			272
7		−8		−32			4			16			4			16
8							−4			−16			4			16
9		−12		−24		−4	−3		−16	−6		4	3		16	6
10													8			32
Sum	−64	−68	−192	−128	−16	0	$-\frac{7}{2}$	−64	16	−4	16	64	$\frac{295}{2}$	64	240	468

The columns labelled by $E^{(1)}\varkappa^n/\varepsilon\Omega$ [see eq (3 28)] yield the Ω^{-2} contributions which arise from the inclusion of the perturbed energy in the denominators corresponding to the diagrams of fig 16 The columns labelled by x^n/Ω contain the contributions to the coefficients $a_{n,1}$.

TABLE 8

The contributions to the coefficients $a_{n,2}$ corresponding to the transition matrix element of the operator Q between the ground state and the one-phonon state, in units of $\frac{1}{128}$ (diagrams of fig. 17)

Graph	x^2/Ω^2	$\frac{(q_1+q_{\bar{1}})^2}{x^2/\Omega^2}$	$\frac{(q_1-q_{\bar{1}})^2}{x^2/\Omega^2}$	$\frac{(q_1+q_{\bar{1}})^4}{x/\Omega^2}$	$\frac{(q_1+q_{\bar{1}})^4}{x^2/\Omega^2}$	$\frac{(q_1{}^2-q_{\bar{1}}{}^2)^2}{x/\Omega^2}$	$\frac{(q_1{}^2-q_{\bar{1}}{}^2)^2}{x^2/\Omega^2}$	$\frac{(q_1-q_{\bar{1}})^4}{x/\Omega^2}$	$\frac{(q_1-q_{\bar{1}})^4}{x^2/\Omega^2}$
1	4	−4	−4						
2	2	$\frac{3}{2}$	$-\frac{3}{2}$	$\frac{1}{2}$	$\frac{1}{4}$	−1	$-\frac{1}{2}$	$\frac{1}{2}$	$\frac{1}{4}$
3		1	−1		$-\frac{1}{2}$				$\frac{1}{2}$
4		1	−1		$-\frac{1}{2}$				$\frac{1}{2}$
5		4	−4						
6					$\frac{1}{2}$		−1		$\frac{1}{2}$
7					$\frac{1}{2}$		−1		$\frac{1}{2}$
8		$\frac{5}{2}$	$-\frac{5}{2}$	$\frac{1}{2}$	$\frac{1}{8}$	−1	$-\frac{1}{4}$	$\frac{1}{2}$	$\frac{1}{8}$
9		1	−1		$-\frac{1}{2}$				$\frac{1}{2}$
10		1	−1		$-\frac{1}{2}$				$\frac{1}{2}$
11					$\frac{1}{8}$		$-\frac{1}{4}$		$\frac{1}{8}$
12							−1		1
13							−1		1
14					$\frac{1}{2}$		−1		$\frac{1}{2}$
15					$\frac{1}{2}$		−1		$\frac{1}{2}$
16							−1		1
17							−1		1
Sum	6	8	−16	1	$\frac{1}{2}$	−2	−9	1	$\frac{17}{2}$

butions yield

$$\langle \mathrm{S}|Q|\mathrm{g\,s}\rangle_{\mathrm{e}}^{(2)} = (2\Omega)^{\frac{1}{2}} q \left(\frac{x}{\Omega^2}\left(\tfrac{3}{16}+\tfrac{53}{64}x\right) + \frac{x(q_1+q_{\bar{1}})^2}{\Omega^2}\left(\tfrac{7}{32}+\tfrac{17}{128}x\right) \right.$$
$$- \frac{x(q_1-q_{\bar{1}})^2}{\Omega^2}\left(\tfrac{15}{32}+\tfrac{339}{128}x\right) + \frac{(q_1+q_{\bar{1}})^4}{32\Omega^2}\left(1-\tfrac{1}{2}x+\tfrac{3}{32}x^2\right)$$
$$\left. - \frac{(q_{\bar{1}}^2-q_1^2)^2}{16\Omega^2}\left(1+\tfrac{7}{2}x+\tfrac{231}{32}x^2\right) + \frac{(q_1-q_{\bar{1}})^4}{32\Omega^2}\left(1+\tfrac{15}{2}x+\tfrac{1099}{32}x^2\right)\right) \quad (3\,29)$$

The total effective matrix element is obtained (up to order Ω^{-2}) adding (3.27), (3 29) and the results of tables 7 and 8

$$\langle \mathrm{S}|Q|\mathrm{g.s.}\rangle_{\mathrm{e}} = (2\Omega)^{\frac{1}{2}} q \left(1+\tfrac{1}{4}x+\tfrac{5}{32}x^2 - \frac{x}{4\Omega} - \frac{17x^2}{32\Omega} + \frac{3x}{16\Omega^2} + \frac{x^2}{2\Omega^2}\right.$$
$$-(q_1+q_{\bar{1}})^2\left(\frac{1}{4\Omega}+\frac{7x^2}{256\Omega}-\frac{5x^2}{128\Omega^2}\right) + (q_1-q_{\bar{1}})^2$$
$$\times\left(\frac{1}{8\Omega}+\frac{x}{2\Omega}+\frac{295x^2}{256\Omega}-\frac{x}{4\Omega^2}-\frac{223x^2}{128\Omega^2}\right) + (q_1+q_{\bar{1}})^4\frac{x^2}{1024\Omega^2}$$
$$\left.+(q_1-q_{\bar{1}})^4\frac{161x^2}{1024\Omega^2} - (q_1^2-q_{\bar{1}}^2)^2\frac{17x^2}{512\Omega^2} + \mathrm{O}(x^3,\Omega^{-3})\right). \quad (3.30)$$

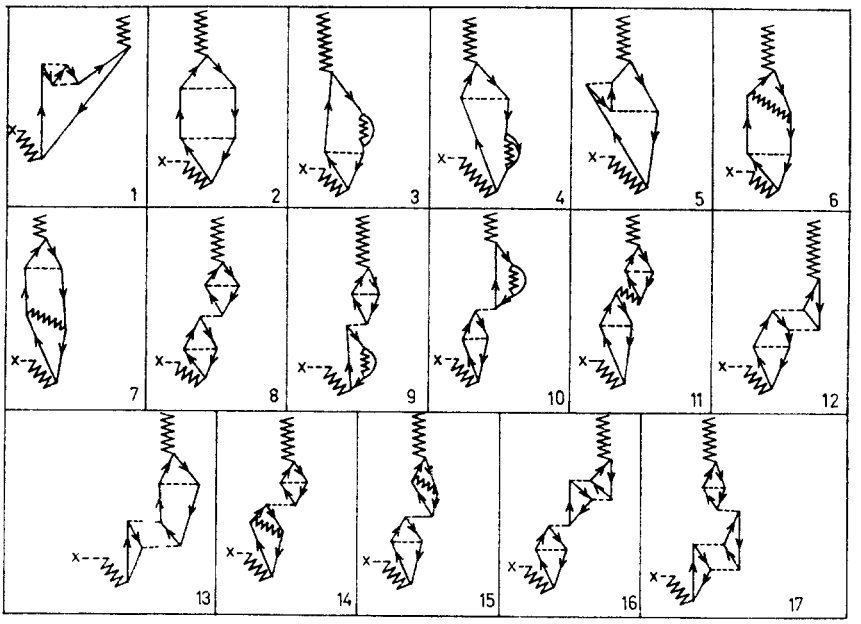

Fig 17 Diagrams contributing to the order Ω^{-2} in the matrix element of the operator Q corresponding to the transition between the ground state and the one-phonon state (see text)

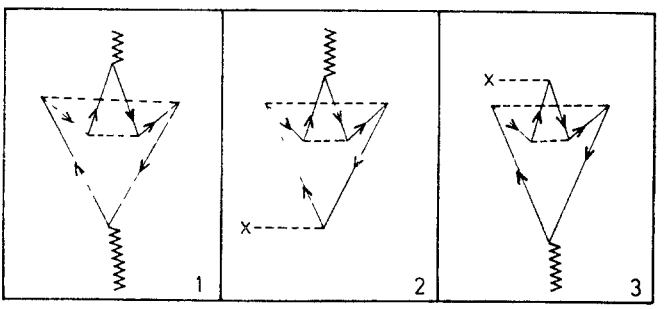

Fig 18 An example of how to obtain the Ω^{-2} contributions to the matrix element of the operator Q corresponding to the vertices from the energy diagrams of the same order

The amplitude of the unperturbed state in the final state is obtained from the partial derivative

$$\frac{\partial W(E)}{\partial E} = \frac{3x}{4\Omega}(1+\tfrac{2}{3}x)+\frac{(q_1+q_{\bar{1}})^2}{4\Omega}(1-\tfrac{1}{4}x)-\frac{(q_1-q_{\bar{1}})^2}{4\Omega}(1+\tfrac{15}{4}x+\tfrac{29}{4}x^2)$$
$$-\frac{3x}{8\Omega^2}(1+\tfrac{9}{4}x)-\frac{x(q_1+q_{\bar{1}})^2}{16\Omega^2}(1+\tfrac{9}{8}x)+\frac{x(q_1-q_{\bar{1}})^2}{16\Omega^2}(9+\tfrac{449}{8}x)$$
$$-\frac{(q_1+q_{\bar{1}})^4}{64\Omega^2}(1-\tfrac{1}{2}x-\tfrac{1}{16}x^2)-\frac{(q_1-q_{\bar{1}})^4}{64\Omega^2}(1+\tfrac{15}{2}x+\tfrac{751}{16}x^2)$$
$$+\frac{(q_1^2-q_{\bar{1}}^2)^2}{32\Omega^2}(1+\tfrac{7}{2}x+\tfrac{119}{16}x^2). \qquad (3\,31)$$

Thus, the amplitude is

$$\left(1-\frac{\partial W(E)}{\partial E}\right)^{-\frac{1}{2}} = 1+\frac{3x}{8\Omega}(1+\tfrac{2}{3}x)+\frac{(q_1+q_{\bar{1}})^2}{8\Omega}(1-\tfrac{1}{4}x)-\frac{(q_1-q_{\bar{1}})^2}{8\Omega}(1+\tfrac{15}{4}x+\tfrac{29}{4}x^2)$$
$$-\frac{3x}{16\Omega^2}(1+\tfrac{9}{8}x)+\frac{7x}{64\Omega^2}(q_1+q_{\bar{1}})^2(1+\tfrac{3}{14}x)+\frac{x}{64\Omega^2}(q_1-q_{\bar{1}})^2(9+\tfrac{145}{2}x)$$
$$+\frac{(q_1+q_{\bar{1}})^4}{64\Omega^2}(1-\tfrac{1}{2}x+\tfrac{1}{8}x^2)+\frac{(q_1-q_{\bar{1}})^4}{64\Omega^2}(1+\tfrac{155}{2}x+\tfrac{1555}{8}x^2)$$
$$-\frac{(q_1^2-q_{\bar{1}}^2)^2}{32\Omega^2}(1+\tfrac{7}{2}x+\tfrac{233}{4}x^2)+O(x^3,\Omega^{-3}). \quad (3\,32)$$

The product of (3.30) and (3.32) yields the final matrix element $\langle S|Q|g\,s.\rangle$ which has the same coefficients $a_{n,m}(q_1, q_{\bar{1}})$ as the ones obtained in the fermion calculation (table 4), at least for $n \leqq 2$ and $m \leqq 2$

3.3.2. Inclusion of the antisymmetrized vertices in the construction of the phonon. The graphical representation of these vertices is obtained from fig 11 by collapsing the dashed lines into a single point Thus fig 11 5 disappears The corresponding values of the vertices are

$$(m_3\,1;\,m_2\,\bar{1}|\bar{H}'_q|m_4\,\bar{1};\,m_1\,1) = \langle \mathrm{HF}|c^+_{m_4\bar{1}}\,c_{m_3 1}\,H'_q\,c^+_{m_1 1}\,c_{m_2\bar{1}}|\mathrm{HF}\rangle$$
$$= -V(\delta_{m_1m_2}\delta_{m_3m_4}-q_{\bar{1}}\,q_1\,\delta_{m_1m_3}\delta_{m_2m_4}) \qquad \text{(fig 11.1)},$$
$$(m_3\,\bar{1};\,m_2\,\bar{1}|\bar{H}'_q|m_4\,1;\,m_1\,1) = \langle \mathrm{HF}|H'_q\,c^+_{m_1 1}\,c_{m_2\bar{1}}\,c^+_{m_4 1}\,c_{m_3\bar{1}}|\mathrm{HF}\rangle$$
$$= -V(\delta_{m_1m_2}\delta_{m_3m_4}-\delta_{m_1m_3}\delta_{m_2m_4}) \qquad \text{(fig 11 2)},$$
$$(m_3\,1;\,m_2\,\bar{1}|\bar{H}'_q|m_4\,1;\,m_1\,1) = \langle \mathrm{HF}|c_{m_3 1}\,H'_q\,c^+_{m_4 1}\,c^+_{m_1 1}\,c_{m_2\bar{1}}|\mathrm{HF}\rangle$$
$$= -Vq_1(\delta_{m_1m_2}\delta_{m_3m_4}-\delta_{m_1m_3}\delta_{m_2m_4}) \qquad \text{(fig 11 3)},$$
$$(m_3\,\bar{1};\,m_2\,\bar{1}|\bar{H}'_q|m_4\,\bar{1};\,m_1\,1) = \langle \mathrm{HF}|c^+_{m_4 1}\,H'_q\,c_{m_3\bar{1}}\,c^+_{m_1 1}\,c_{m_2\bar{1}}|\mathrm{HF}\rangle$$
$$= Vq_{\bar{1}}(\delta_{m_1m_2}\delta_{m_3m_4}-\delta_{m_1m_3}\delta_{m_2m_4}) \qquad \text{(fig 11.4)},$$
$$(m_2\,1,\,m_3\,1|\bar{H}'_q|m_4\,1:\,m_1\,1) = \langle \mathrm{HF}|c_{m_2 1}\,c_{m_3 1}\,H'_q\,c^+_{m_1 1}\,c^+_{m_4 1}|\mathrm{HF}\rangle$$
$$= -Vq_1^2(\delta_{m_1m_3}\delta_{m_2m_4}-\delta_{m_1m_2}\delta_{m_3m_4}) \qquad \text{(fig. 11.6)},$$
$$(m_2\,\bar{1};\,m_3\,\bar{1}|\bar{H}'_q|m_4\,\bar{1};\,m_1\,\bar{1}) = \langle \mathrm{HF}|c^+_{m_4\bar{1}}\,c^+_{m_1\bar{1}}\,H'_q\,c_{m_3\bar{1}}\,c_{m_2\bar{1}}|\mathrm{HF}\rangle$$
$$= -Vq_{\bar{1}}^2(\delta_{m_1m_3}\delta_{m_2m_4}-\delta_{m_1m_2}\delta_{m_3m_4}) \qquad \text{(fig. 11.7)}.$$

It is convenient to classify the particle-hole states $c^+_{m1}c_{m'\bar{1}}|0\rangle$ by the magnetic quantum number M

$$M = m-m', \qquad (3.34)$$

since the RPA equations separate for each value of M:

$$(\varepsilon-\omega_{M,\nu})\lambda^{(M)}_{\nu,m}+\sum_{m'}(m1;\,m'-M\bar{1}|\bar{H}'_q|m-M\bar{1};\,m'1)\lambda^{(M)}_{\nu,m'}$$
$$+\sum_{m'}(m1;\,m'1|\bar{H}'_p|m-M\bar{1};\,m'+M\bar{1})\mu^{(M)}_{\nu,m'}=0, \quad (3.35)$$
$$(\varepsilon+\omega_{M,\nu})\mu^{(M)}_{\nu,m}+\sum_{m'}(m1;\,m'-M\bar{1}|\bar{H}'_q|m-M\bar{1};\,m'1)\mu^{(M)}_{\nu,m'}$$
$$+\sum_{m'}(m1;\,m'1|\bar{H}'_p|m-M\bar{1};\,m'+M\bar{1})\lambda^{(M)}_{\nu,m'}=0.$$

The RPA bosons are given by the linear combinations

$$\Gamma^{+}_{M,\nu}=\sum_{m}(\lambda^{(M)}_{\nu,m}c^{+}_{m+M1}\,c_{m\bar{1}}-\mu^{(M)}_{\nu,m}c^{+}_{m+M\bar{1}}\,c_{m1}). \quad (3.36)$$

If $M=0$, there are two RPA roots $\omega_{0,\nu}$ The first one, ω, corresponds to the adiabatic phonon ($\nu=1$), and is obtained by taking the amplitudes $\lambda^{(0)}_{1,m}$ and $\mu^{(0)}_{1,m}$ to be independent of m. Thus, (3.35) reads

$$\begin{aligned}(\varepsilon'-\omega-V(2\Omega-1))\lambda-V(2\Omega-1)\mu&=0,\\ -V(2\Omega-1)\lambda+(\varepsilon'+\omega-V(2\Omega-1))\mu&=0,\end{aligned} \quad (3.37)$$

where

$$\varepsilon'=\varepsilon+Vq_1q_{\bar{1}}-V. \quad (3.38)$$

Eq. (3 37) yields the energy

$$\omega=\varepsilon\left(1-x+\frac{x}{4\Omega}(2q_1q_{\bar{1}}+x-xq_1q_{\bar{1}})-\frac{x^2}{16\Omega^2}(1-q_1^2q_{\bar{1}}^2)\right)^{\frac{1}{2}}$$
$$=\varepsilon\left(1-\tfrac{1}{2}x-\tfrac{1}{8}x^2-\tfrac{1}{16}x^3+\frac{1}{\Omega}(\tfrac{1}{8}x^2+\tfrac{1}{16}x^3)-\frac{1}{\Omega^2}(\tfrac{1}{32}x^2+\tfrac{1}{64}x^3)\right.$$
$$\left.+\frac{q_1q_{\bar{1}}}{\Omega}(\tfrac{1}{4}x+\tfrac{1}{32}x^3)-\frac{q_1q_{\bar{1}}}{\Omega^2}\frac{x^3}{32}\right)+O(x^4,\Omega^{-3}). \quad (3.39)$$

The amplitudes are

$$\lambda=\lambda^{(0)}_{1,m}=\tfrac{1}{2}(2\Omega)^{-\frac{1}{2}}((\varepsilon'/\omega)^{\frac{1}{2}}+(\omega/\varepsilon')^{\frac{1}{2}})=(2\Omega)^{-\frac{1}{2}}\left(1+\tfrac{1}{32}x^2-\frac{x^2}{32\Omega}+O(x^3,\Omega^{-3})\right),$$
$$\mu=\mu^{(0)}_{1,m}=\tfrac{1}{2}(2\Omega)^{-\frac{1}{2}}((\varepsilon'/\omega)^{\frac{1}{2}}-(\omega/\varepsilon')^{\frac{1}{2}}) \quad (3.40)$$
$$=(2\Omega)^{-\frac{1}{2}}\left(\tfrac{1}{4}x+\tfrac{1}{8}x^2-\frac{1}{\Omega}(\tfrac{1}{8}x+\tfrac{1}{16}x^2)-\frac{q_1q_{\bar{1}}}{\Omega}\frac{x^2}{16}+\frac{q_1q_{\bar{1}}}{\Omega^2}\frac{x^2}{32}+O(x^3,\Omega^{-3})\right).$$

The other $2\Omega-1$ solutions for the case $M=0$, and all solutions for $M\neq 0$

(non-adiabatic phonons) yield the frequency ω_M through the equations

$$(\varepsilon' - \omega_M + V)\lambda_{\nu,m}^{(M)} + V\mu_{\nu,m}^{(M)} = 0,$$

$$V\lambda_{\nu,m}^{(M)} + (\varepsilon' + \omega_M + V)\mu_{\nu,m}^{(M)} = 0, \tag{3.41}$$

where ε' is given in (3.38). Thus,

$$\omega_M = \varepsilon\left(1 - \frac{x^2}{16\Omega^2} + \frac{q_1 q_{\bar{1}}}{\Omega}\frac{x}{2} + \frac{q_1^2 q_{\bar{1}}^2}{\Omega^2}\frac{x^2}{16}\right)^{\frac{1}{2}}$$

$$= \varepsilon\left(1 - \frac{x^2}{32\Omega^2} + \frac{q_1 q_{\bar{1}}}{\Omega}\frac{x}{4} + O(x^3, \Omega^{-3})\right). \tag{3.42}$$

The amplitudes $\lambda_{\nu,m}^{(M)}$ and $\mu_{\nu,m}^{(M)}$ of the non-adiabatic bosons may be written

$$\lambda_{\nu,m}^{(M)} = \lambda_M a_{\nu,m}^{(M)}, \qquad \mu_{\nu,m}^{(M)} = \mu_M a_{\nu,m}^{(M)}, \tag{3.43}$$

where the coefficients $a_{\nu,m}^{(M)}$ satisfy the conditions

$$\sum_m a_{\nu,m}^{(0)} = 0 \qquad (\nu > 1),$$

$$a_{\nu,m}^{(M)} = \delta_{\nu,m} \qquad (M \neq 0), \tag{3.44}$$

$$\sum_m |a_{\nu,m}^{(M)}|^2 = 1.$$

The coefficients λ_M and μ_M are given by

$$\lambda_M = \frac{1}{2}\left(\left(\frac{\varepsilon'}{\omega_M}\right)^{\frac{1}{2}} + \left(\frac{\omega_M}{\varepsilon'}\right)^{\frac{1}{2}}\right) = 1 + \frac{x^2}{128\Omega^2} + O(\Omega^{-3}),$$

$$\mu_M = \frac{1}{2}\left(\left(\frac{\varepsilon'}{\omega_M}\right)^{\frac{1}{2}} - \left(\frac{\omega_M}{\varepsilon'}\right)^{\frac{1}{2}}\right) = -\frac{x}{8\Omega} + \frac{x^2 q_1 q_{\bar{1}}}{32\Omega^2} + O(\Omega^{-3}). \tag{3.45}$$

Eqs. (3.39) and (3.45) contain all the RPA results that we need in order to construct the field Hamiltonian The pure boson term is

$$H_b = \omega\Gamma^+\Gamma + \omega_M \sum_{M,\nu}(1 - \delta_{M\,0}\delta_{\nu,1})\Gamma_{M,\nu}^+\Gamma_{M,\nu}, \tag{3.46}$$

where the subindices $M = 0$, $\nu = 1$ are dropped from the adiabatic phonon.

The two-body matrix elements (3 16) are replaced in eq (3 20) by the antisymmetrized ones (3.33), in order to obtain the new particle-vibration interaction vertices

For the adiabatic phonon

$$\Lambda(m'\sigma', m\sigma) = -\Lambda(\sigma', \sigma)\delta_{m,m'},$$

$$\Lambda(1, \bar{1}) = V(2\Omega - q_1 q_{\bar{1}})\lambda + V(2\Omega - 1)\mu$$
$$= \varepsilon(2\Omega)^{-\frac{1}{2}}\left(\tfrac{1}{2}x + \tfrac{1}{8}x^2 - \frac{x^2}{8\Omega} - \frac{q_1 q_{\bar{1}} x}{4\Omega} + O(x^3, \Omega^{-2})\right) \quad \text{(vertex 12.1)},$$

$$\Lambda(\bar{1}, 1) = V(2\Omega - 1)\lambda + V(2\Omega - q_1 q_{\bar{1}})\mu \tag{3.47}$$
$$= \varepsilon(2\Omega)^{-\frac{1}{2}}\left(\tfrac{1}{2}x + \tfrac{1}{8}x^2 - \frac{1}{\Omega}(\tfrac{1}{4}x + \tfrac{1}{16}x^2) - \frac{q_1 q_{\bar{1}}}{\Omega}\frac{x^2}{16} + O(x^3, \Omega^{-2})\right)$$
(vertex 12.2),

$$\Lambda(1, 1) = V q_1(2\Omega - 1)(\lambda + \mu)$$
$$= \varepsilon q_1(2\Omega)^{-\frac{1}{2}}\left(\tfrac{1}{2}x + \tfrac{1}{8}x^2 - \frac{1}{8\Omega}x^2 + O(x^3, \Omega^{-2})\right) \quad \text{(vertex 12.3)},$$

$$\Lambda(\bar{1}, \bar{1}) = -\Lambda(1, 1)(q_{\bar{1}}/q_1) \quad \text{(vertex 12 4)}$$

The particle-vibration vertices corresponding to non-adiabatic phonons are smaller than (3 47) by an order of magnitude in Ω^{-1}, namely,

$$\Lambda_{M,\nu}(m + M1, m\bar{1}) = V(q_1 q_{\bar{1}}\lambda_M + \mu_M)a^{(M)}_{\nu,m}$$
$$= \frac{\varepsilon}{\Omega}a^{(M)}_{\nu,m}\left(q_1 q_{\bar{1}}\frac{x}{4} - \frac{x^2}{32\Omega} + O(x^3, \Omega^{-2})\right) \quad \text{(vertex 12.1)},$$

$$\Lambda_{M,\nu}(m + M\bar{1}, m1) = V(\lambda_M + q_1 q_{\bar{1}}\mu_M)a^{(M)}_{\nu,m}$$
$$= \frac{\varepsilon}{\Omega}a^{(M)}_{\nu,m}\left(\tfrac{1}{4}x - \frac{x^2}{32\Omega}q_1 q_{\bar{1}} + O(x^3, \Omega^{-2})\right) \quad \text{(vertex 12.2)},$$

$$\Lambda_{M,\nu}(m + M1, m1) = q_1 V(\lambda_M + \mu_M)a^{(M)}_{\nu,m} \tag{3.48}$$
$$= \frac{\varepsilon}{\Omega}a^{(M)}_{\nu,m}q_1\left(\tfrac{1}{4}x - \frac{x^2}{32\Omega} + O(x^3, \Omega^{-2})\right) \quad \text{(vertex 12 3)},$$

$$\Lambda_{M,\nu}(m + M\bar{1}, m\bar{1}) = -q_{\bar{1}}/q_1\,\Lambda_{M,\nu}(m + M1, m1) \quad \text{(vertex 12.4)}$$

We construct the particle-vibration interaction term in the field Hamiltonian with the vertices (3 47) and (3 48)

$$H_{p,\nu} = -(\Lambda(1, \bar{1})A^+ + \Lambda(\bar{1}, 1)A + \Lambda(1, 1)N_1 + \Lambda(\bar{1}, \bar{1})N_{\bar{1}})\Gamma$$
$$+ \sum_{\substack{M,\nu\\ \sigma,\sigma'}}(1 - \delta_{M,0}\delta_{\nu,1})\Lambda_{M,\nu}(m + M\sigma, m\sigma')c^+_{m+M\sigma}c_{m\sigma'}\Gamma_{M,\nu}(1 - \delta_{\sigma+\sigma',-2})$$
$$+ \sum_{M,\nu}(1 - \delta_{M,0}\delta_{\nu,1})\Lambda_{M,\nu}(m + M\bar{1}, m\bar{1})c_{m\bar{1}}c^+_{m+M\bar{1}}\Gamma_{M,\nu} + \text{h c.} \tag{3 49}$$

The total field Hamiltonian H_f (3.24) is obtained from (3.14), (3.46) and (3.49). The forbidden "bubbles" are now more general than before, since they can also be generated by vertex 11.5. Consequently, fewer diagrams appear in the graphical expansion. For instance, the diagram 13.3 is now forbidden. Its contribution (table 5) is already included in the energy ω of the adiabatic phonon (eq. (3.39)). We also disregard diagrams 14.11, 14.16 and 14.21: if we add their three values (table 6) plus the renormalization contributions corresponding to graph 14.21, we obtain the Ω^{-2} terms in eq. (3.39).

Similarly, diagram 13.2 yields the value

$$-\frac{\Lambda^2(1,\bar{1})\Lambda(1,1)\Lambda(\bar{1},\bar{1})4\Omega}{\varepsilon(\varepsilon-\omega)^2}-\frac{\Lambda(1,\bar{1})\Lambda(\bar{1},1)(\Lambda^2(1,1)+\Lambda^2(\bar{1},\bar{1}))4\Omega}{\varepsilon(\varepsilon^2-\omega^2)}$$
$$+\frac{\Lambda^2(1,\bar{1})\Lambda^2(\bar{1},1)4\Omega}{\varepsilon(\varepsilon^2-\omega^2)}+O(x^4)=\varepsilon\left(\frac{x^3}{16\Omega}-\frac{x^3}{16\Omega^2}+\frac{(q_1+q_{\bar{1}})^2}{\Omega}\frac{x^2}{16}\right.$$
$$+\frac{(q_1+q_{\bar{1}})^2}{\Omega^2}\left(\tfrac{1}{16}x^2+\tfrac{1}{128}x^3\right)-\frac{(q_1-q_{\bar{1}})^2}{\Omega}\left(\tfrac{1}{16}x^2+\tfrac{1}{16}x^3\right)$$
$$\left.+\frac{(q_1-q_{\bar{1}})^2}{\Omega^2}\left(\tfrac{1}{16}x^2+\tfrac{13}{128}x^3\right)\right)+O(x^4,\Omega^{-3}), \tag{3.50}$$

if the intermediate phonon is the adiabatic one. The value (3.50) is obtained adding the contributions of subsect 3 3.1 corresponding to diagrams 13.2, 14.7, 14.10, 14 22, 14.36 and 14.38 (tables 5 and 6) plus the renormalization permutations corresponding to graph 14.36. The 46 diagrams of fig. 14 are reduced to 16 diagrams when the antisymmetrized vertices (3.33) are used in the construction of the phonon.

Diagram 19.1 presents a fermion line in parallel with a boson line Thus, the last rule listed in sect. 1 for the field theory must be applied. If graph 19.1 is evaluated with the particle-vibration interaction (3.49), the additional diagram 19.2 must be subtracted in order not to count twice the corresponding process. This is due to the existence of two equivalent lines in graph 19.2. The contribution of fig. 19, where

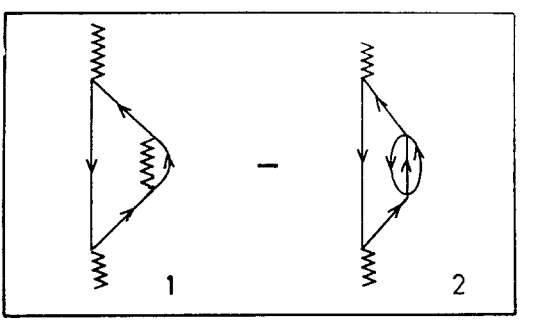

Fig 19. An example of a graph with a particle and a phonon line in parallel (1) and the corresponding graph to be subtracted (2)

the intermediate boson is either adiabatic or non-adiabatic, accounts for the diagrams 13 1, 14.1, 14 9, 14.13, 14 17, 14.18, 14.20 and 14 23 of the previous subsection

The total contribution of the non-adiabatic phonons in the case of graph 19.1 is as large as the contribution of the adiabatic phonon Unlike in subsect. 3 3.1, the non-adiabatic phonons now appear because the frequency ω_M is different from ε, and thus the coupling constants (3 48) do not vanish

The obvious advantage of including antisymmetrized vertices in the construction of the phonon, is to decrease the number of existing diagrams in a given graphical expansion However, the procedure of subsect 3 3.1 may be preferred when the interaction becomes separable for the direct components because (i) the RPA equations are simpler to solve, (ii) if we include the exchange vertices in the definition of the boson, both parameters ω and Λ are given by an expansion in powers of Ω^{-1}, the leading order terms being Ω^0 and $\Omega^{-\frac{1}{2}}$ respectively. Thus, each graph does not correspond to a single power of Ω^{-1}, (iii) there is no need to subtract an additional graph whenever there is a diagram in which a fermion line and a phonon line appear and disappear at the same vertices (such as in fig 19)

4. Conclusions

We have performed the field treatment of residual nuclear interactions in simple but non-trivial models, which include most of the complexities of real nuclei. Calculations concerning energies and transition matrix elements have been presented

In zero order, both the independent particle and the collective aspects of the nucleon motion are included on the same footing The errors introduced by considering too many degrees of freedom are corrected in successive orders of perturbation The (diagrammatic) field treatment corresponds to an expansion in powers of Ω^{-1}, where Ω measures the number of particle-hole or particle-particle components in the phonons A calculation which includes all the Ω^{-1} corrections appears to be feasible in actual nuclei, both for schematic and realistic forces. Indeed, we have treated in subsect. 3 3 2 the problem of a non-separable interaction, by including the exchange components of the force in the construction of the phonon

Note that diagrams such as 20 3 and 20.4 have not been taken into account in the particle-vibration calculations that have been published so far. Thus none of these calculations appear to be sufficiently accurate (even up to the order Ω^{-1})

The shell-model degeneracies are such that corrections of order Ω^{-1} will be in general sufficient Both the number and the complexity of the diagrams involved in a calculation of order Ω^{-2} become very large and such calculations can only be performed for very specific cases

Discussions with A. Bohr, P. F. Bortignon, E E Maqueda, T. Marumori, B Mottelson, R. P J. Perazzo and A. Toledo Piza are gratefully acknowledged.

Appendix A

THE MATRIX ELEMENTS OF THE FERMION HAMILTONIANS (2 10) AND (3 14)

The construction of these matrices is greatly simplified because the relevant operators obey the commutation relations of a SU(2) algebra in both cases. In the pairing case, we notice

$$[A_\sigma^+, A_\sigma] = N_\sigma - \Omega,$$
$$[\tfrac{1}{2}(N_\sigma - \Omega), A_\sigma^+] = A_\sigma^+. \tag{A.1}$$

Therefore, the operators A_σ^+, A_σ and $\frac{1}{2}(N_\sigma - \Omega)$ obey the same commutation relations as I_+, I_- and I_z. Using the quasispin formalism, it is easy to construct the matrix elements of A_σ^+ in the representation which carries $N_\sigma(I_z)$ as good quantum number. Since $0 \leqq N \leqq 2\Omega$, the largest representation have $I = \frac{1}{2}\Omega$ (even system) and $I = \frac{1}{2}(\Omega - 1)$ (odd system):

$$\langle N'_\sigma | A_\sigma^+ | N_\sigma \rangle = (I + \tfrac{1}{2}(\Omega - N_\sigma))^{\frac{1}{2}} (I + \tfrac{1}{2}(N_\sigma - \Omega) + 1)^{\frac{1}{2}} \delta_{N'_\sigma, N_\sigma + 2}$$
$$= \tfrac{1}{2}\delta_{N'_\sigma, N_\sigma + 2} \times \begin{cases} ((2\Omega - N_\sigma)(N_\sigma + 2))^{\frac{1}{2}} & (N_\sigma, \text{ even}) \\ ((2\Omega - N_\sigma - 1)(N_\sigma + 1))^{\frac{1}{2}} & (N_\sigma, \text{ odd}). \end{cases} \tag{A 2}$$

Using (A.2), we construct the matrix element

$$\langle N'_\sigma | (A_\sigma^+ A_\sigma + A_\sigma A_\sigma^+) | N_\sigma \rangle = \tfrac{1}{2}\delta_{N'_\sigma, N_\sigma} \times \begin{cases} 2\Omega N_\sigma + 2\Omega - N_\sigma^2 & (N_\sigma, \text{ even}) \\ 2\Omega N_\sigma - 1 - N_\sigma^2 & (N_\sigma, \text{ odd}). \end{cases} \tag{A 3}$$

Eqs. (A.2) and (A.3) yield the non-vanishing matrix elements of H'_p (eq. (2.10) in a representation in which both N_1 and $N_{\bar{1}}$ are good quantum numbers We assume N_σ to be even in (A.4) while $N_{\bar{\sigma}}$ may be even or odd,

$$\langle N_\sigma, N_{\bar{\sigma}} | H'_p | N_\sigma, N_{\bar{\sigma}} \rangle$$
$$= -\tfrac{1}{2}G \langle N_\sigma, N_{\bar{\sigma}} | (A_1^+ A_1 + A_1 A_1^+ + A_{\bar{1}}^+ A_{\bar{1}} + A_{\bar{1}} A_{\bar{1}}^+ + N_1 + N_{\bar{1}}) | N_\sigma N_{\bar{\sigma}} \rangle$$
$$= \tfrac{1}{4}G(N_\sigma^2 + N_{\bar{\sigma}}^2) - \tfrac{1}{2}G(\Omega + 1)(N_\sigma + N_{\bar{\sigma}}) - \begin{cases} G\Omega & (N_{\bar{\sigma}}, \text{ even}) \\ \tfrac{1}{4}G(2\Omega - 1) & (N_{\bar{\sigma}}, \text{ odd}). \end{cases} \tag{A.4}$$

$$\langle N_\sigma + 2, N_{\bar{\sigma}} + 2 | H'_p | N_\sigma, N_{\bar{\sigma}} \rangle = -G \langle N_\sigma + 2, N_{\bar{\sigma}} + 2 | A_1^+ A_{\bar{1}}^+ | N_\sigma, N_{\bar{\sigma}} \rangle$$
$$= -\tfrac{1}{4}G((2\Omega - N_\sigma)(N_\sigma + 2))^{\frac{1}{2}} \times \begin{cases} ((2\Omega - N_{\bar{\sigma}})(N_{\bar{\sigma}} + 2))^{\frac{1}{2}} & (N_{\bar{\sigma}}, \text{ even}) \\ ((2\Omega - N_{\bar{\sigma}} - 1)(N_{\bar{\sigma}} + 1))^{\frac{1}{2}} & (N_{\bar{\sigma}}, \text{ odd}). \end{cases} \tag{A.5}$$

We proceed similarly with the monopole force [3]) The commutation relations between the operators A^+, A and $\frac{1}{2}(N_1 + N_{\bar{1}} - 2\Omega)$ [eq. (3 5)] are now the same as those of I_+, I_- and I_z,

$$[A^+, A] = N_1 + N_{\bar{1}} - 2\Omega, \qquad [\tfrac{1}{2}(N_1 + N_{\bar{1}} - 2\Omega), A^+] = A^+. \tag{A.6}$$

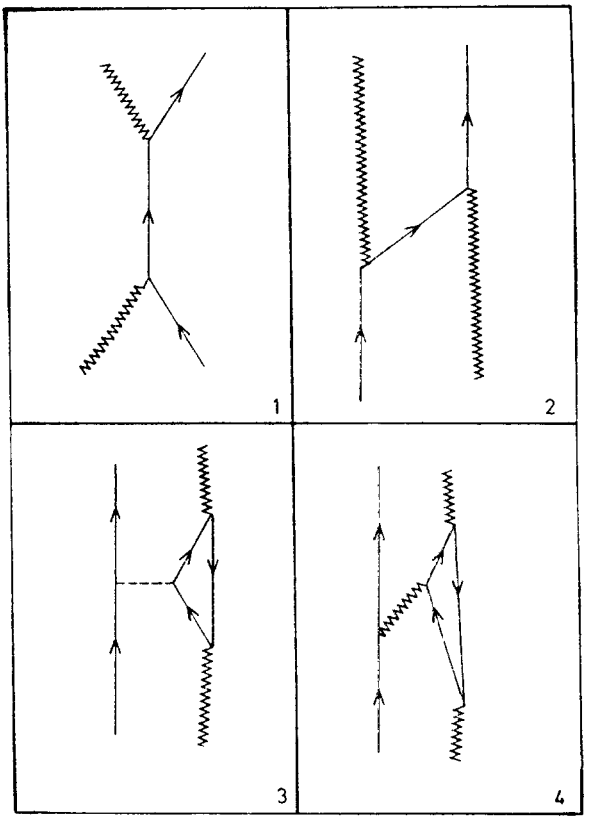

Fig. 20 Diagrams corresponding to the order Ω^{-1} in the energy of a particle-phonon state.

As in (A.2) or in ref [3]), we can evaluate the matrix elements of A^+,

$$\langle N'|A^+|N\rangle = \delta_{N',N+1}(2\Omega-N)^{\frac{1}{2}}(N+1)^{\frac{1}{2}},$$

$$\langle m'\sigma'; N'|A^+|m\sigma; N\rangle = \delta_{m,m'}\delta_{\sigma,\sigma'}\delta_{N',N+1}(2\Omega-N-1)^{\frac{1}{2}}(N+1)^{\frac{1}{2}}, \qquad \text{(A.7)}$$

where N is the number of particle-hole pairs and $m\sigma$ are the quantum numbers of the odd particle or hole

Using (A.7) it is easy to calculate the non-vanishing matrix elements of (3.14) when $N_1 = N_{\bar{1}}$,

$$\langle N+2|H'_q|N\rangle = -\tfrac{1}{2}V((2\Omega-N)(2\Omega-N-1)(N+1)(N+2))^{\frac{1}{2}}, \qquad \text{(A.8)}$$

$$\langle N+1|H'_q|N\rangle = -V(q_1-q_{\bar{1}})N(2\Omega-N)^{\frac{1}{2}}(N+1)^{\frac{1}{2}}, \qquad \text{(A.9)}$$

$$\langle N|H'_q|N\rangle = -V(N(2\Omega-N+1)+\tfrac{1}{2}N(N-1)(q_1-q_{\bar{1}})^2-Nq_1q_{\bar{1}}). \qquad \text{(A.10}$$

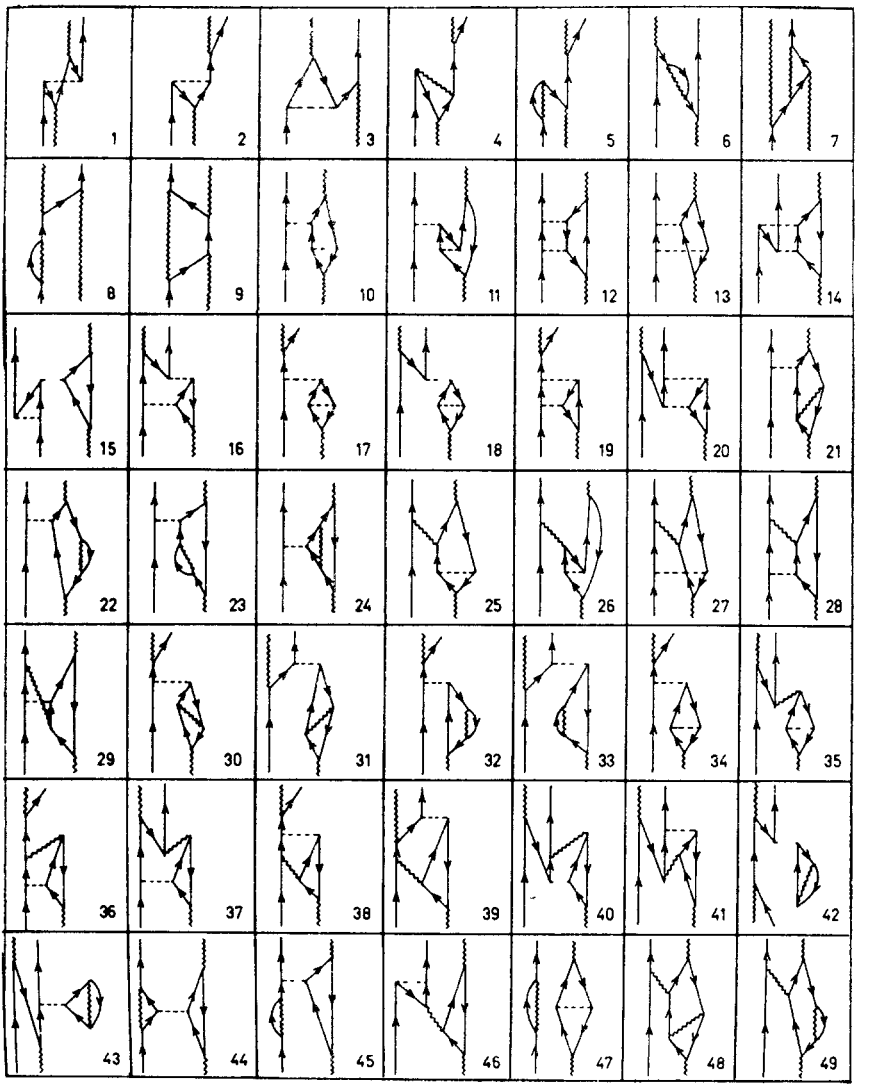

Fig 21. Diagrams corresponding to the order Ω^{-2} in the energy of a particle-phonon state

If $N_1 = N_{\bar{1}} \pm 1$, we obtain

$$\langle m\sigma; N+2|H_q'|m\sigma; N\rangle = -\tfrac{1}{2}V((2\Omega-N-1)(2\Omega-N-2)(N+1)(N+2))^{\frac{1}{2}}, \quad \text{(A.11)}$$

$$\langle m\sigma; N+1|H_q'|m\sigma; N\rangle = -V(N(q_1-q_{\bar{1}})+\sigma q_\sigma)((2\Omega-N-1)(N+1))^{\frac{1}{2}}, \quad \text{(A.12)}$$

$$\langle m\sigma; N|H_q'|m\sigma; N\rangle = -V(2N\Omega-N^2+\tfrac{1}{2}N^2(q_1-q_{\bar{1}})^2-\tfrac{1}{2}N(q_1+q_{\bar{1}})^2+Nq_\sigma^2). \quad \text{(A.13)}$$

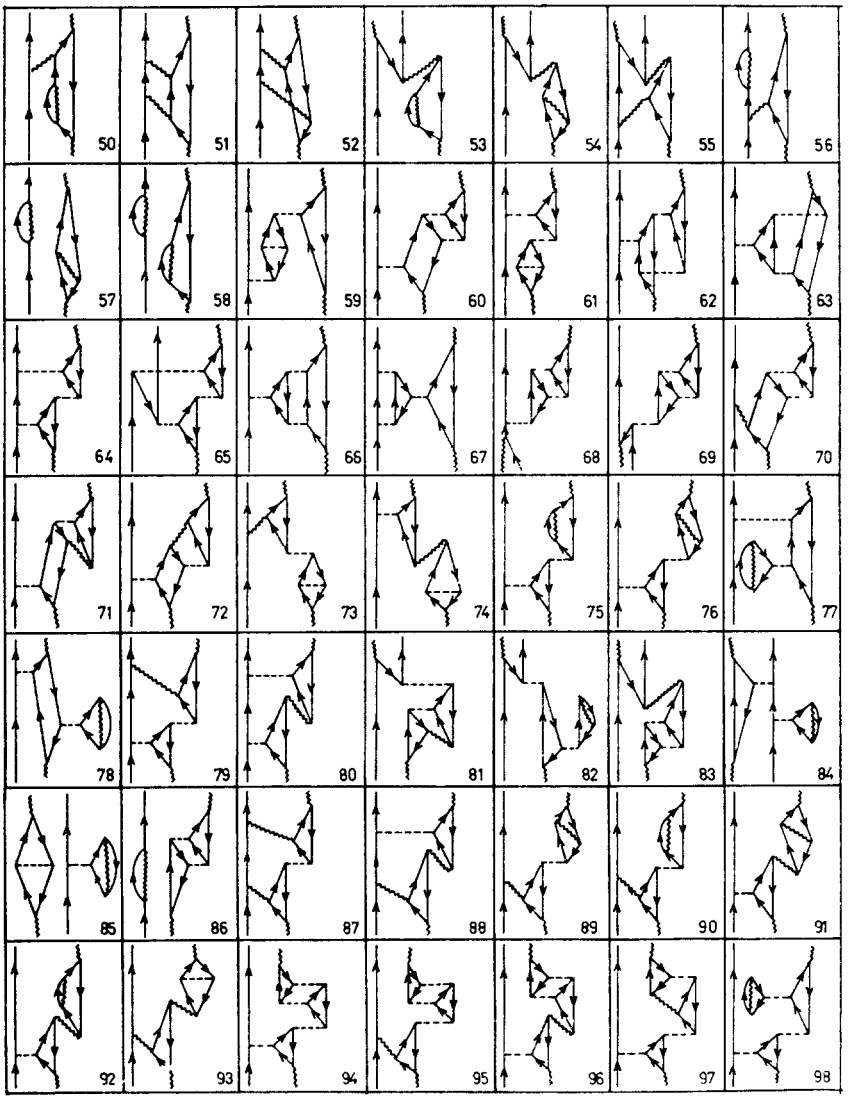

Fig. 21 (continued)

TABLE 9

The contributions of the diagrams in fig. 20 to the coefficients $a_{n,1}$ (in units of $\frac{1}{128}$)

				$(q_1+q_{\bar{1}})^2$			$q_1{}^2-q_{\bar{1}}{}^2$			$(q_1-q_{\bar{1}})^2$		
	x	x^2	x^3	x	x^2	x^3	x	x^2	x^3	x	x^2	x^3
1		8	6		4	4		8	8		4	4
2	32	8	6		−4	−4		− 8	− 8		− 4	− 4
3							−16	−16	−10	−16	−16	−10
4								−16	−32		−16	−32
Sum	32	16	12	0	0	0	−16	−32	−42	−16	−32	−42

TABLE

The contributions of the diagrams in fig. 21

				$(q_1+q_{\bar{1}})^2$			$q_1^2-q_{\bar{1}}^2$			$(q_1-q_{\bar{1}})^2$		
	x	x^2	x^3	x	x^2	x^3	x	x^2	x^3	x	x^2	x^3
1	−16		−2	4		$\frac{1}{2}$	8	8	5	4	8	$\frac{9}{2}$
2		−8	−4		−4	$-\frac{9}{2}$		−8	−8		−4	$-\frac{7}{2}$
3		−8	−4	−8	4	$\frac{7}{2}$		8	8	8	4	$\frac{9}{2}$
4			−4			−1			−2			−1
5												
6		−4	−4		2			−4			2	4
7			−4		−8				8		8	12
8		−8	−8		4	3		8	6		4	7
9		−4	−4		4	3		8	14		4	11
10								12	10		12	10
11								8	4		8	4
12		−8	−2			2						2
13			−4		−4	6			4		4	2
14					8	−4		8	4		8	4
15								8	8		8	8
16							16	12	2	16	12	6
17			−4		−2	$-\frac{5}{2}$			−4		2	$-\frac{3}{2}$
18		−16	−4	−8	2	$\frac{3}{2}$			4	8	−2	$\frac{5}{2}$
19								4			4	2
20									8		16	6
21									10			10
22								4	$\frac{9}{2}$		4	$\frac{9}{2}$
23								4	11		4	11
24									$\frac{13}{2}$			$\frac{13}{2}$
25									12			12
26									8			8
27						−8						8
28			−8			4			4			4
29			−4			12			12			12
30						−2						2
31			−8		−8	2					8	6
32			−4						−4			
33		−16	−12		8				4		8	16
34						−1						1
35			−6		−2	$-\frac{3}{2}$					2	$\frac{3}{2}$
36									2			2
37								4	11		4	11
38									4			4
39								16	28		16	28
40									3			17
41									−3			17
42									$-\frac{5}{2}$			$\frac{5}{2}$
43									5			5
44									$\frac{11}{2}$			$\frac{13}{2}$
45								4	7		4	11
46									8			8
47			−2		−2	$-\frac{1}{4}$			2		2	$\frac{9}{4}$
48												
49									4			4
50									4			4
51												
52												

to the coefficients $a_{n,2}$ (in units of $\frac{1}{128}$)

$(q_1+q_{\bar{1}})^4$			$(q_1+q_{\bar{1}})^3(q_1-q_{\bar{1}})$			$(q_1^2-q_{\bar{1}}^2)^2$			$(q_1+q_{\bar{1}})(q_1-q_{\bar{1}})^3$			$(q_1-q_{\bar{1}})^4$		
x	x^2	x^3	x	x^2	x^3	x	x^2	x^3	x	x^2	x^3	x	x^2	x^3
			4	1		4	1		−4	−1		−4	−1	
					1			1			−1			−1
−2	$\frac{5}{2}$	$\frac{1}{2}$	−4	5	1	−4	1	−1	−4	−3	−3	−2	$-\frac{3}{2}$	$-\frac{3}{2}$
2	$-\frac{5}{2}$	$\frac{1}{2}$	4	−5	1		−4		−4	−3	−1	−2	$-\frac{3}{2}$	$-\frac{1}{2}$
		−1			−2			−2			−2			−1
				−2	−1		−6	−3		−6	−3		−2	−1
	−1	$-\frac{1}{2}$		−2	−1					2	1		1	$\frac{1}{2}$
	1	$\frac{1}{2}$		2	1					−2	−1		−1	$-\frac{1}{2}$
				2	2		6	6		6	6		2	2
					−1			−3			−3			−1
				4	3		4	3		−4	−5		−4	−5
				2	$-\frac{5}{2}$		2	$-\frac{5}{2}$		−2	$-\frac{7}{2}$		−2	$-\frac{7}{2}$
				−6	1		−6	1		−2	−3		−2	−3
					$-\frac{3}{2}$			$-\frac{3}{2}$			$-\frac{1}{2}$			$-\frac{1}{2}$
				4	5		4	5		−4	−5		−4	−5
	4	−1		8	−2			−8		−8	−14		−4	−7
	−4	2		−8	4		−8	−4		−8	−12		−4	−6
		−1			−2			−2			−2			−1
		−1			−2						2			1
		1			2						−2			−1
		1			2			2			2			1
		−1			−2			−2			−2			−1
		$-\frac{1}{4}$			$-\frac{1}{2}$						$\frac{1}{2}$			$\frac{1}{4}$
		$\frac{3}{4}$			$\frac{3}{2}$						$-\frac{3}{2}$			$-\frac{3}{4}$
					$\frac{1}{2}$			$\frac{3}{2}$			$\frac{3}{2}$			$\frac{1}{2}$
					$-\frac{3}{2}$			$-\frac{9}{2}$			$-\frac{9}{2}$			$-\frac{3}{2}$
					2			6			6			2
					−2			−6			−6			−2
					$-\frac{1}{2}$			$-\frac{3}{2}$			$-\frac{3}{2}$			$-\frac{1}{2}$
				−2	$-\frac{5}{2}$		−6	$-\frac{15}{2}$		−6	$-\frac{15}{2}$		−2	$-\frac{5}{2}$
	1	1		2	2					−2	−2		−1	−1
					4			4			−4			−4
					2			2			−2			−2
					−6			−6			−2			−2
		−2			−4			−4			−4			−2
		2			4						−4			−2

TABLE 10

				$(q_1+q_{\bar{1}})^2$			$q_2^1-q_{\bar{1}}^2$			$(q_1-q_{\bar{1}})^2$		
	x	x^2	x^3	x	x^2	x^3	x	x^2	x^3	x	x^2	x^3
53			−4			2						2
54						−2						2
55									4			4
56									4			4
57						−2						2
58			−4			4			4			4
59									4			4
60									8			8
61								8	8		8	8
62									8			8
63												
64												
65												17
66									5			5
67												5
68												4
69											16	
70												
71												
72												
73									8			8
74									3			3
75								8	12		8	12
76									4			4
77												
78												
79												
80												
81												32
82												12
83												4
84												
85												
86												4
87												
88												
89												
90									8			8
91												
92									2			2
93												
94												
95												
96												
97												
98												
Sum(p)	−16	−72	−100	−12	2	$\frac{59}{4}$	24	120	299	36	182	$\frac{1897}{4}$
Ren	16	52	62	12	2	$-\frac{15}{4}$	−24	−80	−157	−36	−130	$-\frac{1085}{4}$
Sum	0	−20	−38	0	4	11	0	40	142	0	52	203

The row labelled by Sum(p) is the sum of rows 1–98. The last row is the sum of the two previous labelled by Renor

(continued)

$(q_1+q_{\bar{1}})^4$			$(q_1+q_{\bar{1}})^3(q_1-q_{\bar{1}})$			$(q_1^2-q_{\bar{1}}^2)^2$			$(q_1+q_{\bar{1}})(q_1-q_{\bar{1}})^3$			$(q_1-q_{\bar{1}})^4$		
x	x^2	x^3	x	x^2	x^3	x	x^2	x^3	x	x^2	x^3	x	x^2	x
					-2			-6			-6			-2
		1			2						-2			-1
		-1			-2			-2			-2			-1
					1			1			-1			-1
										-8	-5		-8	-5
			4	2	$\frac{1}{2}$	4	2	$\frac{1}{2}$	-4	-2	$-\frac{1}{2}$	-4	-2	$-\frac{1}{2}$
											-4			-4
					3			3			-3			-3
						-4	-6	$-\frac{9}{2}$	-8	-12	-9	-4	-6	$-\frac{9}{2}$
					-3			-3			-3			-3
								-3			-6			-3
								2			4			2
								-2			-4			-2
											-8			-8
					$\frac{3}{2}$			$\frac{3}{2}$			$-\frac{17}{2}$			$-\frac{17}{2}$
					$-\frac{3}{2}$			$-\frac{3}{2}$			$-\frac{17}{2}$			$-\frac{17}{2}$
				4	6		4	6		-4	-6		-4	-6
				1	$\frac{5}{2}$		1	$\frac{5}{2}$		-1	$-\frac{5}{2}$		-1	$-\frac{5}{2}$
				-4	-2		-4	-2		-4	-10		-4	-10
				4	2		4	2		-4	-6		-4	-6
					$-\frac{5}{2}$			$-\frac{5}{2}$			$-\frac{5}{2}$			$-\frac{5}{2}$
					$\frac{5}{2}$			$\frac{5}{2}$			$-\frac{5}{2}$			$-\frac{5}{2}$
							-8	-20		-16	-40		-8	-20
							-1	$-\frac{9}{2}$		-2	-9		-1	$-\frac{9}{2}$
								$-\frac{5}{2}$			-5			$-\frac{5}{2}$
					$\frac{5}{4}$			$\frac{5}{4}$			$-\frac{5}{4}$			$-\frac{5}{4}$
								-2			-4			-2
								-4			-8			-4
								-2			-4			-2
					4			4			-4			-4
					-4			-4			-4			-4
					1			1			-1			-1
					-1			-1			-1			-1
					1			1			-1			-1
										-8	-6		-8	-6
											-8			-8
											-2			-2
											-17			-17
											-5			-5
0	1	$\frac{3}{2}$	8	12	$\frac{61}{4}$	0	-20	$-\frac{261}{4}$	-24	-104	$-\frac{1197}{4}$	-16	-73	$-\frac{881}{4}$
0	-1	$-\frac{3}{2}$	-8	-12	$-\frac{53}{4}$	0	20	$\frac{245}{4}$	24	104	$\frac{1093}{4}$	16	73	$\frac{801}{4}$
0	0	0	0	0	2	0	0	-4	0	0	-26	0	0	-20

rows. Thus, it also includes the contributions from renormalization graphs, which are given in the row

Appendix B

EVALUATION OF THE GROUND-STATE ENERGY WITHIN THE RPA APPROXIMATION

Within the RPA approximation, the Hamiltonian (2.10) can be written

$$H_{\mathrm{RPA}} = \varepsilon(A_1^+A_1 + A_{\bar{1}}^+A_{\bar{1}}) - \tfrac{1}{2}G(A_1^+ + A_{\bar{1}})(A_1 + A_{\bar{1}}^+) - \tfrac{1}{2}G(A_{\bar{1}}^+ + A_1)(A_{\bar{1}} + A_1^+). \quad \text{(B.1)}$$

In order to calculate the ground-state energy, we use the inverse RPA transformation

$$A_1^+ = \sqrt{\Omega}(\lambda\Gamma_1^+ + \mu\Gamma_{\bar{1}}), \qquad A_{\bar{1}}^+ = \sqrt{\Omega}(\lambda\Gamma_{\bar{1}}^+ + \mu\Gamma_1), \quad \text{(B.2)}$$

where the coefficients λ and μ are given in (2 14). Replacing (B.2) in (B.1) leads to

$$H_{\mathrm{RPA}} = (2\lambda\mu\varepsilon - G\Omega(\lambda+\mu)^2)(\Gamma_1^+\Gamma_{\bar{1}}^+ + \Gamma_1\Gamma_{\bar{1}}) + (\varepsilon(\lambda^2+\mu^2) - G\Omega(\lambda+\mu)^2)(\Gamma_1^+\Gamma_1 + \Gamma_{\bar{1}}^+\Gamma_{\bar{1}}) + 2\varepsilon\mu^2 - G\Omega(\lambda+\mu)^2. \quad \text{(B.3)}$$

The coefficient of the first term in (B 3) vanishes for the RPA values (2 14). The second term is the frequency ω (2.13) and the third one, the ground-state energy This can also be written as

$$\langle\psi|H_{\mathrm{RPA}}|\psi\rangle = 2\varepsilon\mu(\mu-\lambda) = -\frac{x\varepsilon^2}{\varepsilon+\omega} = -\tfrac{1}{2}x\varepsilon(1+\tfrac{1}{4}x+\tfrac{1}{8}x^2+\tfrac{5}{64}x^3+\ .\ \ ). \quad \text{(B.4)}$$

Appendix C

THE PARTICLE-PHONON STATE

The state which has a particle and a phonon has played a crucial role in the history of the particle-vibration interaction Thus, we treat this case in detail, using the methods of subsect 3 3.1.

The zero-order excitation energy is again the frequency ω (eq. (3 24)), which agrees with the Ω^0 terms of table 4. The first-order contributions are given in fig 20 and table 9 and the second-order terms, in fig 21 and table 10 These results reproduce those of the fermion calculation (table 4)

References

1) D. R. Bès, R A Broglia, G G Dussel, R J Liotta and B. R Mottelson, Phys Lett **52B** (1974) 253
2) D. R Bès, R A Broglia, G G Dussel, R J Liotta and R P J Perazzo, Nucl. Phys **A260** (1976) 77
3) D R. Bès, R A Broglia, G G Dussel, R J Liotta and H M Sofía, Nucl. Phys **A260** (1976) 1
4) P. Nozières, Theory of interacting Fermi systems (Benjamin, New York, 1964)
5) G. Alaga, V. Paar and L. Sips, ed., Proc. Topical Conf on problem of vibrational nuclei, Zagreb, 1974 (North-Holland, Amsterdam, 1975)